102324

WATER RESOURCES RESEARCH, VOL. 29, NO. 1, PAGES 17–33, JANUARY 1993

Exact Scheffé-Type Confidence Intervals for Output From Groundwater Flow Models 1. Use of Hydrogeologic Information

RICHARD L. COOLEY

Water Resources Division, U.S. Geological Survey, Denver, Colorado

A new method is developed to efficiently compute exact Scheffé-type confidence intervals for output (or other function of parameters) $g(\beta)$ derived from a groundwater flow model. The method is general in that parameter uncertainty can be specified by any statistical distribution having a log probability density function (log pdf) that can be expanded in a Taylor series. However, for this study parameter uncertainty is specified by a statistical multivariate beta distribution that incorporates hydrogeologic information in the form of the investigator's best estimates of parameters and a grouping of random variables representing possible parameter values so that each group is defined by maximum and minimum bounds and an ordering according to increasing value. The new method forms the confidence intervals from maximum and minimum limits of $g(\beta)$ on a contour of a linear combination of (1) the quadratic form for the parameters used by Cooley and Vecchia (1987) and (2) the log pdf for the multivariate beta distribution. Three example problems are used to compare characteristics of the confidence intervals for hydraulic head obtained using different weights for the linear combination. Different weights generally produced similar confidence intervals, whereas the method of Cooley and Vecchia (1987) often produced much larger confidence intervals.

INTRODUCTION

The degree of uncertainty in results of a groundwater flow model is dependent upon the degree of uncertainty in information on aquifer properties and other quantities (collectively termed parameters) used to construct it. It is well known [e.g., *Dettinger and Wilson*, 1981] that this information is generally uncertain. This uncertainty is caused mainly by inaccuracies and inadequacies in methods of obtaining estimates for true values of the parameters and by uncertainty in the spatial (and sometimes temporal) variability of the true values. Use of single or fixed estimates of parameters that are, in reality, uncertain produces model output quantities, such as hydraulic heads and fluxes, that are uncertain to an unknown degree and thus unreliable. Therefore to produce a more reliable model it is necessary to replace the single estimates of parameters with a statistical distribution that expresses the known degree of uncertainty about the true values of the parameters. Then, this distribution of potential candidates for true values of the parameters (referred to here simply as the distribution of parameters) should be used to produce a distribution of model output quantities that expresses the degree of uncertainty in output from the model [*Konikow*, 1986, p. 183].

In general, the model output quantities are nonlinear functions of the parameters, which makes analysis of uncertainty in model output difficult [*Dettinger and Wilson*, 1981; *Cooley and Vecchia*, 1987]. The principal approaches that have been used to characterize uncertainty in model output resulting from uncertainty and spatial variability of parameters were briefly reviewed by *Cooley and Vecchia* [1987]. These approaches were categorized as linearization methods, which compute variances of desired model output based on linearizations of model equations, and Monte Carlo methods, which approximate the statistical distribution of model output by performing numerous model runs. Comprehensive reviews of stochastic methods of incorporating spatial variability of parameters into the theory and analysis of groundwater flow and transport have recently been presented by *Dagan* [1986] and *Gelhar* [1984, 1986]. Application of the methods reviewed by these authors to computing variances and covariances of model output quantities for practical problems again appears to be confined to the linearization and Monte Carlo methods. Both of these methods have serious drawbacks. Use of linearization methods is restricted to systems characterized by small parameter variances, and Monte Carlo methods are computationally intensive.

If the assessment of uncertainty in model output is to have a probabilistic basis, then confidence and prediction intervals for model output should be computed. A confidence interval for some function of parameters, such as model output, is a range of the function such that there is a specified probability that the true value of the function lies within the range [*Graybill*, 1976, p. 86]. In contrast, a prediction interval is a range of a random variable corresponding to the function such that there is a specified probability that a future observation of the random variable lies within the range [*Graybill*, 1976, pp. 267–268]. The random variable for prediction intervals is generally formed by adding a random error (or noise) component to the function of parameters. Both types of intervals can be computed using the statistical distribution, variances, and covariances of the function, but the statistical distribution, variances, and covariances of the errors are also required for prediction intervals.

Approximate confidence and prediction intervals for model output can be computed by linearizing the model [*Seber and Wild*, 1989, pp. 191–196; *Cooley and Naff*, 1990, pp. 172–176]. In this case, variances and covariances of the model output can easily be computed, and the statistical distributions of model output can usually be derived, at least in approximate form. In addition, this method can be ex-

This paper is not subject to U.S. copyright. Published in 1993 by the American Geophysical Union.

Paper number 92WR01863.

31119

tended to obtain confidence intervals for other nonlinear functions of parameters that might be of interest [*Seber and Wild*, 1989, p. 192]. However, parameter variances must generally be small for the intervals to be good approximations. Better approximations would be obtained using the Monte Carlo method or a reparameterization method such that the reparameterized function has statistical properties that are similar to those of a linear function [*Bates*, 1992]. Only the Monte Carlo method fully accounts for nonlinearity, and as indicated above, it is computationally intensive.

Computation of confidence and prediction intervals that fully account for the nonlinearity can also be approached as a constrained, nonlinear optimization problem. *Cooley and Vecchia* [1987] developed a method of computing these types of intervals and applied it using specific bounded parameter and model error distributions that were considered to reflect commonly available knowledge of parameters and model errors. However, the method ignored the bounds and so produced intervals that were often conservative (too wide) [*Hill*, 1989].

Widths of confidence and prediction intervals depend on the assumed statistical distribution of parameters. If the model were fitted to available data (termed calibration data) such as observed hydraulic heads and fluxes, then it would probably be observed that certain combinations of parameter values produce poor fits of the model to the data. In these cases the calibration data indicate that these combinations of parameter values are unlikely. A statistical distribution of parameters that does not directly incorporate model fit to the calibration data (such as the one used by *Cooley and Vecchia* [1987]) could easily have a variance-covariance structure that allows these combinations to be likely, whereas a statistical distribution of parameters that incorporates model fit to the calibration data would have a variance-covariance structure that makes these combinations unlikely. This reduction of likelihood would reduce the sizes of computed confidence and prediction intervals.

Part 1 of this study describes a new method of calculating exact confidence intervals using the statistical parameter distribution of *Cooley and Vecchia* [1987]. The methods are applied to three example problems to analyze the quality of, and major influences on, the confidence intervals. In part 2 [*Cooley*, this issue] a method of incorporating calibration data is developed and applied to the second and third example problems of part 1.

Prediction intervals are not included in either of the two parts. However, the method of *Cooley and Vecchia* [1987] for computing them can easily be adapted to the new methods.

METHODS OF CONSTRUCTING CONFIDENCE INTERVALS

Assumed Distribution for Parameters

Definitions of quantities relating to the distribution of model parameters are similar to those used by *Cooley and Vecchia* [1987]. Assume that a fixed but unknown set of true parameters $\boldsymbol{\beta}$ exists. Also define $\tilde{\mathbf{b}}$ equal to a fixed estimate of $\boldsymbol{\beta}$ resulting from prior (measured and subjective) information and (or) model calibration and $\mathbf{B}$ equal to a set of random variables from a statistical distribution that describes parameter uncertainty and covers the plausible range for $\boldsymbol{\beta}$; $\boldsymbol{\beta}$ and $\tilde{\mathbf{b}}$ are regarded as possible realizations of $\mathbf{B}$.

For this study the statistical distribution assumed for $\mathbf{B}$ is the one used by *Cooley and Vecchia* [1987], and this distribution is termed the prior distribution. Extreme values and ordering of the parameters are assumed to have been obtained from measurements and other (perhaps subjective) hydrogeological information, possibly augmented by the model calibration process. Ordering of the parameters is accomplished by identifying parameters that can be grouped so that the parameters in each group form an ordered sequence. Thus parameters are assumed to exist in k independent groups. The p_l parameters in the lth group ($l = 1, 2, \cdots, k$) form the ordered sequence

$$L_l \le b_{l1} \le b_{l2} \le \cdots \le b_{lj} \le \cdots \le b_{lp_l} \le U_l \tag{1}$$

where b_{lj} is a realization of B_{lj}, B_{lj} is an element of vector $(B_{l1}, B_{l2}, \cdots, B_{lp_l})^T = \mathbf{B}_l$, $\mathbf{B}_l$ is a subvector of vector $(\mathbf{B}_1^T, \mathbf{B}_2^T, \cdots, \mathbf{B}_k^T)^T = \mathbf{B}$, L_l is the lower bound for the group, and U_l is the upper bound for the group.

The probability density function (pdf) for the distribution used by *Cooley and Vecchia* [1987] can be stated for each group in the form (A. V. Vecchia, unpublished manuscript, 1991)

$$f_{\mathbf{B}_l}(\mathbf{b}_l) = \frac{(b_{l1} - L_l)^{m_{l1}-1}}{(U_l - L_l)^{m_{l,p_l+1}-1}} \prod_{j=1}^{p_l} \frac{(b_{l,j+1} - b_{lj})^{n_{lj}-1}}{B(m_{lj}, n_{lj})} \tag{2}$$

$$L_l \le b_{l1} \le \cdots \le b_{lp_l} \le U_l$$

where $B(m_{lj}, n_{lj})$ is the standard beta function, $b_{l,p_l+1} = U_l$, and m_{lj} and n_{lj} are distributional parameters that satisfy $m_{lj} > 0$, $n_{lj} > 0$, and

$$m_{l,j+1} = m_{lj} + n_{lj} \tag{3}$$

Specific definitions for m_{lj} and n_{lj} are given by *Cooley and Vecchia* [1987, p. 587] as

$$m_{lj} = \left(\frac{1 - c_l^*}{c_l^*}\right) \frac{\hat{b}_{lj} - L_l}{U_l - L_l} \tag{4}$$

$$n_{lj} = \left(\frac{1 - c_l^*}{c_l^*}\right) \frac{\hat{b}_{l,j+1} - \hat{b}_{lj}}{U_l - L_l} \tag{5}$$

where

$$c_l^* = \frac{c}{p_l + 2} \tag{6}$$

$$\hat{b}_{lj} = E(B_{lj}) \tag{7}$$

In (6), c is a parameter that determines the peakedness of the distribution (the smaller the value of c, the more peaked the distribution) and must satisfy $0 < c \le 1$ [*Cooley and Vecchia*, 1987, p. 587]. In (7), $E(\ )$ indicates the expected value operator. Because the parameter groups are statistically independent, the pdf for the distribution of all groups is

$$f_{\mathbf{B}}(\mathbf{b}) = \prod_{l=1}^{k} f_{\mathbf{B}_l}(\mathbf{b}_l) \tag{8}$$

The marginal distribution of each of the elements B_{lj} corresponding to (2) is a univariate beta distribution given by

Cooley and Vecchia [1987, p. 587]. Therefore (2) (and, by extension, (8)) will henceforth be referred to as a multivariate beta distribution.

Cooley and Vecchia [1987] assumed that $\bar{\mathbf{b}}$ was equivalent to $\hat{\mathbf{b}}$, the mean value of $\mathbf{B}$. However, in an actual modeling situation, $\bar{\mathbf{b}}$ is interpreted as the set most likely to be close to the true parameter set $\boldsymbol{\beta}$. Hence for this study we assume that $\bar{\mathbf{b}}$ is the mode of (8). Because of the asymmetry of (8), the mode $\bar{\mathbf{b}}$ may be different from the mean $\hat{\mathbf{b}}$. It is shown in Appendix A that $\hat{\mathbf{b}}$ and $\bar{\mathbf{b}}$ are related by

$$\hat{b}_{lj} = \frac{(1-c)(\bar{b}_{lj} - L_l) + jc_l^*(U_l - L_l)}{1 - c_l^*} + L_l \qquad (9)$$

Note that when $c = 1$ the mode drops out of (9). This case is an ordered uniform distribution [*Cooley and Vecchia*, 1987, p. 584] which has no unique mode.

Finally, as shown by *Cooley and Vecchia* [1987, pp. 587–588],

$$\begin{aligned} \mathrm{Cov}\,(B_{li}, B_{lj}) &= c_l^*(\hat{b}_{li} - L_l)(U_l - \hat{b}_{lj}) \qquad i \le j \\ \mathrm{Cov}\,(B_{li}, B_{lj}) &= c_l^*(\hat{b}_{lj} - L_l)(U_l - \hat{b}_{li}) \qquad i > j \end{aligned} \qquad (10)$$

where Cov (,) is the covariance operator. Note that Cov (B_{lj}, B_{lj}) = Var (B_{lj}), where Var ( ) is the variance operator. The full parameter variance-covariance matrix can be written as

$$\mathrm{Var}\,(\mathbf{B}) = \mathrm{diag}\,(\mathrm{Var}\,(\mathbf{B}_1), \cdots, \mathrm{Var}\,(\mathbf{B}_l), \cdots, \mathrm{Var}\,(\mathbf{B}_k)) \qquad (11)$$

where the block diagonal form results from the k independent groups of parameters and Var $(\mathbf{B}_l)$ is a $p_l \times p_l$ matrix with the (i, j)th element given by (10). For future compactness define

$$\mathbf{V} = \mathrm{Var}\,(\mathbf{B}) \qquad (12)$$

$$\mathbf{V}_l = \mathrm{Var}\,(\mathbf{B}_l) \qquad (13)$$

The multivariate beta distribution is not required for the general methods developed by this study. It was adopted for the specific methods used because of its versatility in describing the type of information that is normally available about model parameters for a modeling study. Its versatility results from use of the peakedness parameter c, parameter grouping, and parameter bounds (L_l, U_l). For example, by setting $c = 1$, the distribution of each parameter group is ordered uniform [*Cooley and Vecchia*, 1987, p. 584]. By varying the grouping, model parameters can be independent, be completely interdependent, or have any degree of interdependence desired. If parameter bounds are unknown, they can be set to yield a large range so that the resulting distribution is essentially unbounded. If the peakedness parameter is also set to a small value (approximately $c \le 0.01$), a distribution that is close to multivariate normal is obtained (R. L. Cooley, unpublished manuscript, 1991). Finally, parameters for this distribution can be log transformed so that the resulting distribution is close to multivariate lognormal. The principal limitations in versatility are that strict ordering of parameters within each group is required and that the variance-covariance structure for the model parameters cannot be arbitrary because it results from the particular ordering, bounds, peakedness parameter, and parameter set $\bar{\mathbf{b}}$ employed.

A general multivariate normal distribution is a possible alternative to the multivariate beta distribution because it contains no ordering assumptions and its covariance structure is arbitrary. However, for many modeling studies, data of sufficient quantity and quality for the model parameters are not available to obtain a good estimate of the variance-covariance matrix. If these data are available and the ordering assumption is deemed invalid, then a distribution such as the multivariate normal distribution should be used. The method of using the multivariate normal distribution is sketched further on.

A good example of use of the ordering concept is based on the work of *Keidser and Rosbjerg* [1991]. A geostatistically generated transmissivity field was estimated using four alternative inverse methods. Good results were obtained by creating transmissivity zones as bands generally paralleling contour intervals of the data, then estimating the zonal transmissivities using nonlinear least squares. In this case, transmissivity values for the zones form an ordered sequence, so that (2) is a natural distribution to describe the interrelationships among the zonal transmissivities. This idea should apply to any type of parameter data that can be contoured and zoned. A parameter group would thus be composed of the ordered sequence of all zones for the parameter type. Group bounds would either be known or set to yield a large range if unknown. Parameter set $\bar{\mathbf{b}}_l$ would reflect the investigator's best estimate of the set of effective values for the zones, and the peakedness parameter could be adjusted to yield parameter variances that reflect the investigator's uncertainty about $\boldsymbol{\beta}_l$. This parameterization assumes that the general configuration for the spatial distribution of a parameter type is known a priori, but the quantitative value of a parameter at any point is unknown.

Confidence intervals computed using the multivariate beta or any other prior distribution reflect the investigator's understanding of the system and are as subjective as the data used to define the distribution. In part 2 of this study, calibration data are used to modify, and minimize the influence of, the original prior distribution.

Types of Confidence Intervals

Cooley and Vecchia [1987, pp. 582, 583, 588] derived their confidence interval as follows. Define $g(\boldsymbol{\beta})$ equal to a model output or other scalar function of parameters $\boldsymbol{\beta}$ for which a confidence interval is desired. Then, define the quantity $d^2_{1-\alpha}$ by the following probability statement:

$$\mathrm{Prob}\,[Q(\mathbf{B}) \le d^2_{1-\alpha}] = 1 - \alpha \qquad (14)$$

where $1 - \alpha$ is the probability level,

$$Q(\mathbf{B}) = (\mathbf{B} - \hat{\mathbf{b}})^T \mathbf{V}^{-1} (\mathbf{B} - \hat{\mathbf{b}}) = \sum_{l=1}^{k} (\mathbf{B}_l - \hat{\mathbf{b}}_l)^T \mathbf{V}_l^{-1} (\mathbf{B}_l - \hat{\mathbf{b}}_l) \qquad (15)$$

and $\mathbf{B}$ is distributed as given by (8). Strictly speaking, (14) defines $Q(\mathbf{b}) \le d^2_{1-\alpha}$ as a $(1 - \alpha)$ 100% tolerance region for $\mathbf{B}$. However, because $\boldsymbol{\beta}$ is assumed to be a realization of $\mathbf{B}$, the region is interpreted as a $(1 - \alpha)$ 100% confidence region for $\boldsymbol{\beta}$. Based on (14), the potentially conservative

$(1 - \alpha)$ 100% confidence interval for $g(\boldsymbol{\beta})$ given by *Cooley and Vecchia* [1987] may be computed as

$$(\min_{\mathbf{b}} g(\mathbf{b}),\ \max_{\mathbf{b}} g(\mathbf{b})) \tag{16}$$

subject to the constraint

$$Q(\mathbf{b}) = d^2_{1-\alpha} \tag{17}$$

where $Q(\mathbf{b})$ is given by (15) with $\mathbf{B}$ replaced by $\mathbf{b}$. A sufficient requirement for use of (17) instead of the inequality implied by (14) is that the gradient of $g(\mathbf{b})$ with respect to $\mathbf{b}$ be nonzero within the closed region $Q(\mathbf{b}) \le d^2_{1-\alpha}$ so that no extrema lie within this region [*Cooley and Vecchia*, 1987, p. 582]. However, it is only necessary that any local extremum of $g(\mathbf{b})$ for $\mathbf{b}$ within the closed region $Q(\mathbf{b}) \le d^2_{1-\alpha}$ lie between the maximum and minimum values taken by $g(\mathbf{b})$ for $\mathbf{b}$ along the boundary $Q(\mathbf{b}) = d^2_{1-\alpha}$. The confidence interval is potentially conservative because (17) does not guarantee that $\mathbf{b}$ will lie inside of the parameter region given by (1).

The reader will note that the quadratic form (15) is generally used in conjunction with a multivariate normal distribution for $\mathbf{B}$ because (15) is proportional to a contour of the log pdf of this distribution. However, any closed contour in the region over which (8) applies can be used to define a probability statement of the general form of (14) and thus can be used to define a confidence interval. Equation (15) was used by *Cooley and Vecchia* [1987] to define the contour because of its simplicity and because the multivariate beta distribution can be close to normal, as discussed above.

The solution to (16) and (17) was derived by *Cooley and Vecchia* [1987, pp. 582, 583, 588] as a Lagrangian optimization problem in which extreme values of the function

$$L_u(\mathbf{b}, \lambda'_u) = g(\mathbf{b}) + \lambda'_u[d^2_{1-\alpha} - Q(\mathbf{b})] \tag{18}$$

were found with respect to $\mathbf{b}$ and the Lagrange multiplier λ'_u. The solution was obtained using a linearization scheme and is given in iteration form as

$$\mathbf{b}_e = \hat{\mathbf{b}} + \lambda_u \mathbf{V}\mathbf{Z}_0 \tag{19}$$

$$\lambda_u = \pm\left(\frac{d^2_{1-\alpha}}{\mathbf{Z}_0^T\mathbf{V}\mathbf{Z}_0}\right)^{1/2} \tag{20}$$

where

$$\mathbf{Z}_0 = \left.\frac{\partial q}{\partial \mathbf{b}}\right|_{\mathbf{b}=\mathbf{b}_0} \tag{21}$$

$$\lambda_u = \frac{1}{2\lambda'_u} \tag{22}$$

and $\mathbf{b}_0$ is the set of parameters obtained on the previous iteration. Use of the plus sign in (20) yields $\mathbf{b}_e$ corresponding to the upper confidence limit, and use of the minus sign yields $\mathbf{b}_e$ corresponding to the lower confidence limit. The iteration method is considered to have converged when $\mathbf{b}_e \approx \mathbf{b}_0$. Actual implementation of (19) and (20) involves use of a damping parameter to reduce oscillations of computed values in $\mathbf{b}_e$. The algorithm is given by *Cooley and Vecchia* [1987, pp. 588–589] with the exception that here the damping parameter is set to unity on the first iteration. If $g(\mathbf{b})$ is the linear model $g(\mathbf{b}) = g(\hat{\mathbf{b}}) + \mathbf{Z}_0(\mathbf{b} - \hat{\mathbf{b}})$, then (19) and (20) can easily be combined to yield the standard form [*Cooley and Vecchia*, 1987, p. 588]

$$g(\mathbf{b}_e) = g(\hat{\mathbf{b}}) \pm d_{1+\alpha}[\mathrm{Var}\ (g(\mathbf{B}))]^{1/2} \tag{23}$$

where

$$\mathrm{Var}\ (g(\mathbf{B})) = \mathbf{Z}_0^T\mathbf{V}\mathbf{Z}_0 \tag{24}$$

Another confidence interval can be obtained by letting the boundary of a closed region analogous to $Q(\mathbf{b}) \le d^2_{1-\alpha}$ be a log pdf contour, that is, a contour of $-\ln(f_{\mathbf{B}}(\mathbf{b}))$. (Here and elsewhere log pdf means negative log pdf.) This contour can be shown to enclose a smaller volume than any other contour for a given probability level [*Lehmann*, 1986, pp. 330–331]. Thus the confidence region for the parameters defined by this contour is at least as small as the confidence region given by (14). Although it cannot be shown that confidence intervals for arbitrary $g(\boldsymbol{\beta})$ are optimal (smallest in width) for the log pdf contour, they might often be expected to be small because the confidence region for the parameters is smallest. This is shown to be true further on. However, it should be noted that these confidence intervals are generally not much smaller than those based on (14), and in one case considered later the confidence interval based on the log pdf is much larger.

From (2) and (8) the log pdf function analogous to $Q(\mathbf{b})$ can be defined by

$$P'(\mathbf{b}) = -\sum_{l=1}^{k} \{(m_{l1} - 1)\ \ln\ (b_{l1} - L_l) - (m_{l,p_l+1} - 1)\ \ln\ (U_l - L_l) + \sum_{j=1}^{p_l} [(n_{lj} - 1) \cdot \ln\ (b_{l,j+1} - b_{lj}) - \ln B(m_{lj}, n_{lj})]\} \tag{25}$$

Terms that are not functions of $\mathbf{b}$ in (25) have no influence on computed confidence intervals. Hence (25) can be rewritten in the simplified, scaled form

$$P(\mathbf{b}) = -\sum_{l=1}^{k}\sum_{j=0}^{p_l} (n_{lj} - 1)\ \ln\left(\frac{b_{l,j+1} - b_{lj}}{U_l - L_l}\right) \tag{26}$$

where $b_{l0} = L_l$ and $n_{l0} = m_{l1}$. The scaling with respect to group ranges $U_l - L_l$ is employed to keep $P(\mathbf{b})$ positive, which was convenient in programming the method for computer solution.

The log pdf function $P(\mathbf{b})$ can be treated just as $Q(\mathbf{b})$ was to compute a confidence interval for $g(\boldsymbol{\beta})$. However, note that a confidence interval based on $Q(\mathbf{b})$ and a confidence interval based on $P(\mathbf{b})$ can be computed using a single function that is a linear combination of $Q(\mathbf{b})$ and $P(\mathbf{b})$. By using (15) and (26), the function can be defined by

$$S(\mathbf{b}) = \frac{a}{2}\sum_{l=1}^{k} (\mathbf{b}_l - \hat{\mathbf{b}}_l)^T\mathbf{V}_l^{-1}(\mathbf{b}_l - \hat{\mathbf{b}}_l) - b\sum_{l=1}^{k}\sum_{j=0}^{p_l} (n_{lj} - 1)\ \ln\left(\frac{b_{l,j+1} - b_{lj}}{U_l - L_l}\right) \tag{27}$$

where $a \geq 0$ and $b \geq 0$ are constants that define the weight given each function. If $a > 0$ and $b = 0$, only the quadratic form is present, and if $a = 0$ and $b > 0$, only the log pdf function is present. For $a > 0$ and $b > 0$, (27) is a general linear combination of the quadratic form and the log pdf function. Use of (27) in the latter context allows the parameter constraints given by (1) to be incorporated into the computation of a confidence interval based primarily on $Q(\mathbf{b})$. This is accomplished by noting that the log pdf function becomes infinite at a constraint boundary, so that if $b = \varepsilon$, where ε is a small number, and $a \gg \varepsilon$, the contour of $S(\mathbf{b})$ is nearly ellipsoidal except near a constraint boundary where it is just inside the boundary. In this case the log pdf function plays a role similar to that of a penalty function [*Himmelblau*, 1972, chapter 7].

In a fashion analogous to (14), the quantity $s_{1-\alpha}$ may be defined by the probability statement

$$\text{Prob}\,[S(\mathbf{B}) \leq s_{1-\alpha}] = 1 - \alpha \tag{28}$$

from which the confidence interval (16) subject to

$$S(\mathbf{b}) \leq s_{1-\alpha} \tag{29}$$

may be derived. Thus $S(\mathbf{b}) \leq s_{1-\alpha}$ can be interpreted as a $(1 - \alpha)$ 100% confidence region for $\boldsymbol{\beta}$ analogous to $Q(\mathbf{b}) \leq d^2_{1-\alpha}$. As before, if there are no extrema of $g(\mathbf{b})$ for $\mathbf{b}$ inside the region given by (29), or if any extremum of $g(\mathbf{b})$ for $\mathbf{b}$ within this region lies between the maximum and minimum values of $g(\mathbf{b})$ for $\mathbf{b}$ along the boundary $S(\mathbf{b}) = s_{1-\alpha}$, then for computational purposes (29) can be replaced by

$$S(\mathbf{b}) = s_{1-\alpha} \tag{30}$$

It is proven in a more general context in part 2 that the confidence interval defined by (16) and (28) is a Scheffé-type confidence interval analogous to the standard Scheffé confidence interval for a linear regression model [*Graybill*, 1976, pp. 198–200]. A Scheffé-type confidence interval for $g(\boldsymbol{\beta})$ holds simultaneously with confidence intervals for all other functions of parameters (subject to continuity restrictions that allow the functions to be expanded in Taylor series). Thus when applied for a specific function, Scheffé-type confidence intervals are conservative [*Rao*, 1973, p. 240]. An appropriate use of Scheffé-type confidence intervals is to compute one or more of them for one (or more) function $g(\boldsymbol{\beta})$ such as hydraulic head, a model flux, or a model parameter, then interpret the intervals to hold simultaneously with all other possible confidence intervals for hydraulic heads, model fluxes, and combinations of parameters of interest. Calculation of individual and finite numbers of simultaneous confidence and prediction intervals for general functions $g(\boldsymbol{\beta})$ is the subject of ongoing research.

The confidence interval may be computed using a simple Lagrangian scheme analogous to (18):

$$L_p(\mathbf{b}, \lambda'_p) = g(\mathbf{b}) + \lambda'_p[s_{1-\alpha} - S(\mathbf{b})] \tag{31}$$

Solution to (31) is obtained by a variant of Newton iteration and is given in Appendix B. It should be noted that the solution method is general and can be applied to any functions $g(\mathbf{b})$ and $S(\mathbf{b})$ that can be expanded in Taylor series in terms of parameters $\mathbf{b}$. The confidence interval found by solution of (31) is exact in that (1) model nonlinearity and parameter constraints are fully incorporated, and (2) if the confidence interval is used in the simultaneous (Scheffé) sense, the probability level $1 - \alpha$ is exact.

Values for $s_{1-\alpha}$ for the multivariate beta distribution are obtained using the same algorithm as given by *Cooley and Vecchia* [1987, p. 587] except that $s_{1-\alpha}$ replaces $d^2_{1-\alpha}$ and $S(\mathbf{b})$ replaces $Q(\mathbf{b})$. Alternatively, if one desired to obtain a confidence interval based on $Q(\mathbf{b})$ and a multivariate normal distribution of $\mathbf{B}$, $s_{1-\alpha}$ would be given by a value of the cumulative chi-square distribution [*Graybill*, 1976, pp. 135–136]. Specifically, for $a = 2$ and $b = 0$ in (27), $s_{1-\alpha} = \chi^2_{p,1-\alpha}$, where $\chi^2_{p,1-\alpha}$ is the upper $(1 - \alpha) \times 100$ percentile of the cumulative chi-square distribution with $p = \sum_{l=1}^{k} p_l$ degrees of freedom. In this case, variance-covariance matrix $\mathbf{V}$ could be an arbitrary positive definite matrix, and constraints (1) would not be invoked.

Contours $Q(\mathbf{b}) = d^2_{1-\alpha}$ and $P(\mathbf{b}) = s_{1-\alpha}$ for two parameters for which $L = 0 \leq b_1 \leq b_2 \leq 1 = U$ are illustrated in Figures 1*a*–1*c*. In all three figures, $\alpha = 0.05$. Figure 1*a* corresponds to the case where modal values $\bar{b}_j$ $(j = 1, 2)$ are given by $\bar{b}_j = j(U - L)/(p + 1) = j/3$. Direct substitution of this expression into (9) verifies that in this case, $\bar{b}_j = \hat{b}_j$. Because $c = 3/11$, the mass of the distribution is concentrated near the mode so that the entire ellipse $Q(\mathbf{b}) = d^2_{1-\alpha}$ lies inside of the parameter constraint boundary. Note also that the elliptical and log pdf confidence regions are similar in size, shape, and area. However, whether or not this similarity would cause the two types of confidence intervals for $g(\boldsymbol{\beta})$ to be similar for any particular flow model would also depend on values of the gradient $\partial g/\partial \mathbf{b}$ near one or more of the constrained maxima and (or) minima that define the confidence intervals. For Figure 1*b* the mode is $(\bar{b}_1, \bar{b}_2) = (0.1, 0.9)$. By employing (9), the mean is calculated as $(\hat{b}_1, \hat{b}_2) = (0.15122, 0.84878)$. Again, because $c = 3/11$, the mass of the distribution is concentrated near the mode. However, in this case the mean and mode are located near the constraint boundary so that the ellipse extends outside of the constraint boundary and the log pdf contour is located very near two sides of the boundary. Probably because the mean and mode are not widely separated, the two regions are similar. For Figure 1*c* the mode is located in the same place as for Figure 1*b*, but because $c = 0.99$ so that the distribution is nearly uniform, the mean is shifted to $(\hat{b}_1, \hat{b}_2) = (0.33023, 0.66977)$. The large value of c causes the mass to be distributed evenly so that the ellipse is almost entirely outside of the constraint boundary and the log pdf region almost contacts the constraint boundary along two sides of the boundary. The wide separation of the mean and mode coupled with the even distribution of mass causes the two regions to be more dissimilar in size and shape than for the first two examples. Thus confidence intervals for $g(\boldsymbol{\beta})$ could be more dissimilar than for the first two examples, especially if the gradient $\partial g/\partial \mathbf{b}$ is large near one or more of the constrained maxima and (or) minima that define the confidence intervals.

EXAMPLES

In this section, three hypothetical examples are used to illustrate controls on the size and characteristics of the three types of confidence intervals: the quadratic-unconstrained type, which is the solution to (31) with $a = 1$ and $b = 0$ given by (19) and (20), the quadratic-constrained type, which is the solution to (31) with $a = 1$ and $b = \varepsilon$, and the log pdf type,

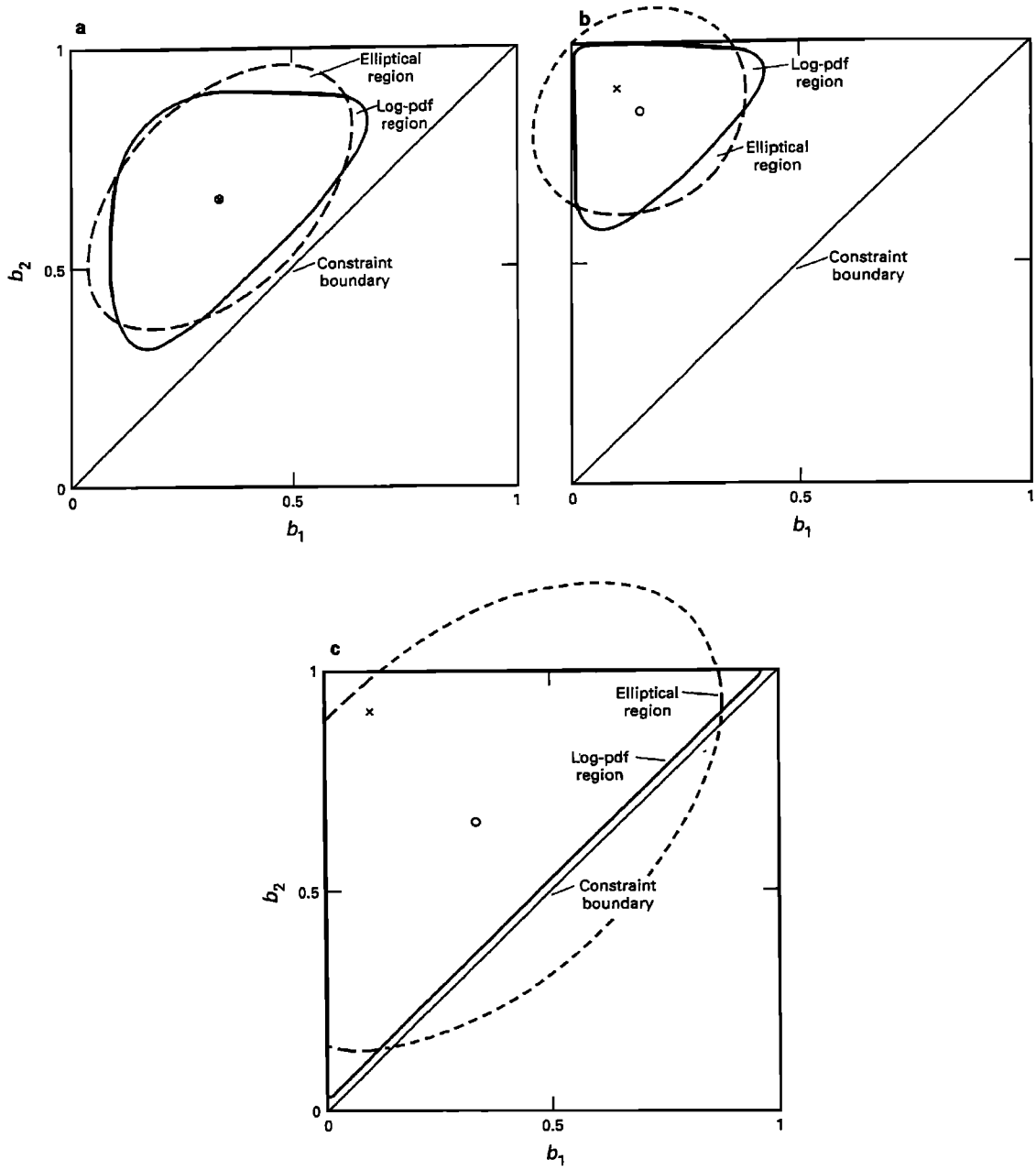

Fig. 1. (*a*) Elliptic ($Q(\mathbf{b}) = d^2_{1-\alpha}$) and log pdf ($P(\mathbf{b}) = s_{1-\alpha}$) contours for a two-parameter region $0 \leq b_1 \leq b_2 \leq 1$, where $c = 3/11$ and the mean (circle) and mode (cross) are equal. (*b*) Elliptic and log pdf contours for the same two-parameter region where $c = 3/11$, but the mean (circle) and mode (cross) are located near the constraint boundary and are separated. (*c*) Elliptic and log pdf contours for the same two-parameter region where $c = 0.99$, which causes the mean (circle) and mode (cross) to be greatly separated.

which is the solution to (31) with $a = 0$ and $b = 1$. A variant of a class of methods known as projection methods [*Himmelblau*, 1972, pp. 245–271] was developed to check the penalty function approach to computing quadratic-constrained confidence intervals and to provide a value for ε. By using $a = 1$ and $\varepsilon = 1 \times 10^{-5}$, the confidence intervals computed by the two methods were virtually identical. Smaller values of ε sometimes caused numerical difficulties because constraint boundaries could be approached so closely that $P(\mathbf{b})$ became very large. Details of the projection method used are available from the author upon request.

One of the controls on sizes of confidence intervals is the assumed value of c. The two values used for testing purposes by *Cooley and Vecchia* [1987] were $c = 3/11$ and $c = 1$, the latter of which corresponds to an ordered uniform distribution. These values were also selected for use here. However, when $c = 1$, combination of (5), (6), and (9) shows that $n_{li} = 1$. Hence, from (26), $P(\mathbf{b}) = 0$, and confidence intervals cannot be computed using the log pdf method. Thus instead of $c = 1$, $c = 0.99$ was used to give an approximation for the ordered uniform distribution. To check this approximation, runs for quadratic-unconstrained and quadratic-constrained intervals (using the projection method) were made using both $c = 1$ and $c = 0.99$. In all instances the difference in width of the confidence intervals for the two values of c was less than 1%, which implies that $c = 0.99$

yields a distribution that is very close to ordered uniform. Therefore when an ordered uniform distribution is assumed, quadratic-constrained and quadratic-unconstrained confidence intervals are based on $c = 1$, and log pdf confidence intervals are based on $c = 0.99$. These intervals are referred to collectively as the $c \approx 1$ case.

A generic system of units was adopted for the examples. Hence lengths and times are not referred to a specific system of units.

Example 1: Flow to a Well in a Homogeneous Aquifer

For the first example a confidence band (a set of confidence intervals) was computed for drawdown near a well pumping from an aquifer receiving uniform recharge. This is the same problem analyzed by *Cooley and Vecchia* [1987, pp. 589–591] and *Hill* [1989, pp. 182–183]. For the problem both pumping rate and recharge are time variant in a stepwise manner. To allow use of a simple analytical solution, the aquifer is assumed to be homogeneous, isotropic, of constant thickness, and infinite in areal extent, and the drawdown is assumed to be small. The solutions for drawdown $g(\boldsymbol{\beta})$ and sensitivities $\partial g/\partial \mathbf{b}$ are given by *Cooley and Vecchia* [1987, pp. 597–598].

Cooley and Vecchia [1987] analyzed a four-parameter, four-group problem where all parameters were considered to be uncorrelated and a four-parameter, three-group problem where the last two parameters were considered to be correlated. Because of the similarity in results, only the four-group problem is considered in detail here. The parameters, their ranges, and pumping and recharge rates are the same as given by *Cooley and Vecchia* [1987]. Parameters and ranges (L_l, U_l) are

$$b_{11} = \ln T \quad \bar{b}_{11} = 6.8024 \quad (L_1, U_1) = (6.5793, 7.0255)$$

$$b_{21} = S_y \quad \bar{b}_{21} = 0.1 \quad (L_2, U_2) = (0.05, 0.15)$$

$$b_{31} = W_2 \quad \bar{b}_{31} = 4 \times 10^{-4}$$

$$(L_3, U_3) = (2.2 \times 10^{-4}, 5.8 \times 10^{-4})$$

$$b_{41} = W_1 \quad \bar{b}_{41} = 6 \times 10^{-4}$$

$$(L_4, U_4) = (5 \times 10^{-4}, 7 \times 10^{-4})$$

where T is transmissivity (length^2/time), S_y is specific yield, W_1 is the recharge rate (length/time) from 0 to 90 time units, and W_2 is the recharge rate (length/time) from 90 to 360 time units, which is the end of the simulation period.

The total simulation period is composed of three pumping periods so that from 0 to 95 time units the pumping rate is zero, from 95 to 180 time units the pumping rate (length^3/time) is 19,008, and from 180 to 360 time units the pumping rate is again zero. A confidence band for drawdown is required for a point 175 length units from the pumped well and 1500 length units from the center of the recharge area, which has a diameter of 10,000 length units.

Cooley and Vecchia [1987] obtained 95% ($\alpha = 0.05$) quadratic-unconstrained confidence bands for $c = 3/11$ and $c = 1$ using the algorithm based on (19) and (20). The bands were constructed from points in time at 1, 30, 60, 90, 105, 120, 150, 180, 190, 210, 240, 270, 300, 330, and 360 time units. It was noted by Cooley and Vecchia that the confidence band for $c = 3/11$ was probably nearly exact because the parameters computed to give max $g(\mathbf{b})$ and min $g(\mathbf{b})$ did not violate their constraints by a significant amount. In contrast, it was noted that the band for $c = 1$ was probably much too conservative because the computed parameters violated their constraints by a large amount. *Hill* [1989] subsequently found by using Monte Carlo simulations that the band for the four-group case using $c = 3/11$ was indeed exact but that the lower bound for the four-group, $c = 1$ band was much too low, often twice as far from the mean as it should be, because of the violation of parameter constraints.

Figure 2 illustrates confidence bands for the four-group, $c = 3/11$ case, and Figure 3 illustrates confidence bands for the four-group, $c \approx 1$ case. The confidence bands may be compared with the results of *Cooley and Vecchia* [1987, p. 592] and *Hill* [1989, p. 183]. Note that in these previous studies the calibrated values were assumed to be the mean $\hat{\mathbf{b}}$, but in the present work they are considered to be the mode $\bar{\mathbf{b}}$. Because for the four-group case the mode for each parameter is centered in its range and all parameters are independent, $\bar{\mathbf{b}} = \hat{\mathbf{b}}$, so there is no difference in numerical values of $\hat{\mathbf{b}}$ used in the former and present studies.

The bands for the $c = 3/11$ and $c = 1$, quadratic-unconstrained cases are the same as the bands obtained by *Cooley and Vecchia* [1987, p. 592]. Figure 2 shows that for $c = 3/11$ the quadratic-unconstrained band is indeed virtually the same as the quadratic-constrained and log pdf bands. Figure 3 shows that for $c = 1$ the lower bound for the quadratic-unconstrained band is often about twice as far from the mode (mean) curve ($g(\mathbf{b})$ as a function of time) as the lower bound for the quadratic-constrained band. This result accords with the result of *Hill* [1989, p. 183] to within the expected accuracy of the Monte Carlo simulations. Finally, note that the quadratic-constrained and log pdf bands for $c \approx 1$ are very similar.

For the three-group case the last two parameters are $b_{31} = W_2$ and $b_{32} = W_1$, and they are correlated, having a range of $(2.2 \times 10^{-4}, 7 \times 10^{-4})$. Thus means $\hat{b}_{31}$ and $\hat{b}_{32}$ had to be calculated from modes $\bar{b}_{31}$ and $\bar{b}_{32}$ using (9). The confidence bands (not illustrated) are almost the same as the bands for the four-group case except that they are a maximum of about 0.3 length units wider (at the widest part of the $c = 1$, quadratic-unconstrained band) than the four-group bands, and the positions of the quadratic-constrained and log pdf bounds for $c \approx 1$ are reversed. This case was not analyzed by *Hill* [1989] so no comparisons with Monte Carlo simulations could be made.

Example 2: One-Dimensional Steady Flow in an Aquifer Having Variable Transmissivity

The second example involves one-dimensional flow in an aquifer where the flux q_B (length^2/time) is known as $q_B = 0.16$ at the inflow end, and the hydraulic head h_B (length) is known as $h_B = 100$ at the outflow end. The aquifer is divided into twenty 1000 length-unit long cells between the inflow and the outflow ends, and each cell has a constant transmissivity. Modal transmissivity values for the cells are given in Table 1, where cell 1 is at the inflow end.

Parameters are the 20 cell values of the log transform, $\ln T$ of transmissivity T. They comprise one group, $L_1 \le b_{11} \le$

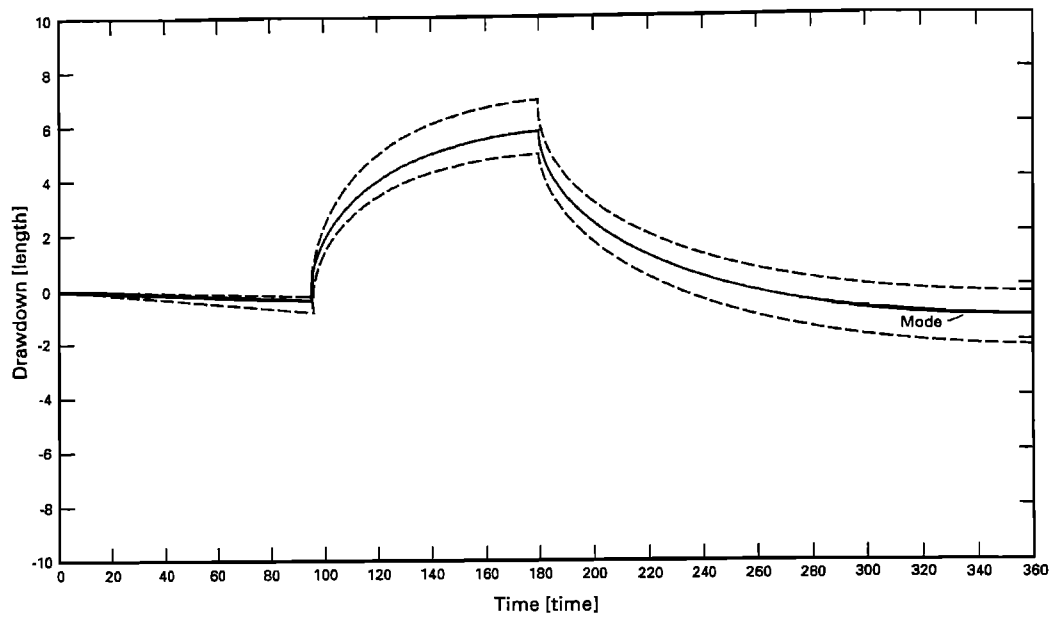

Fig. 2. Ninety-five percent confidence band for drawdown $g(\boldsymbol{\beta})$ for the problem of flow to a well in a homogeneous aquifer (example 1), using $c = 3/11$. The quadratic-unconstrained, quadratic-constrained, and log pdf bands are all nearly the same and are plotted as a single band. The mode is $g(\bar{\mathbf{b}})$.

$b_{12} \leq \cdots \leq b_{1,20} \leq U_1$. Cases considered involve two different assumed ranges (L_1, U_1), two different values of c, and the three types of confidence intervals (log pdf, quadratic constrained, and quadratic unconstrained). These cases, arranged into 12 different model runs, are given in Table 2. Ninety-five percent confidence intervals for the hydraulic head at the inflow end of the aquifer were obtained for all of the model runs.

The method employed to solve for hydraulic heads and sensitivities is the integrated finite difference method described by *Cooley* [1985, p. 1526]. Sensitivities were calculated using the adjoint state sensitivity method given by *Sykes et al.* [1985, pp. 361–362]. Similar implementation of the adjoint state method to compute quadratic-unconstrained confidence intervals based on a different finite difference model is described by *Hill* [1989, pp. 180–181]. For the present example, node points were placed at each cell boundary, giving a total of 21 nodes along the linear aquifer.

For each model run a confidence interval obtained by using the nonlinear model $g(\mathbf{b})$ and a confidence interval obtained by using the linear model (B1) (Appendix B) were both computed. To use (B1) a set of values for the arbitrary parameter set $\mathbf{b}_0$ had to be chosen. The set chosen was $\hat{\mathbf{b}}$

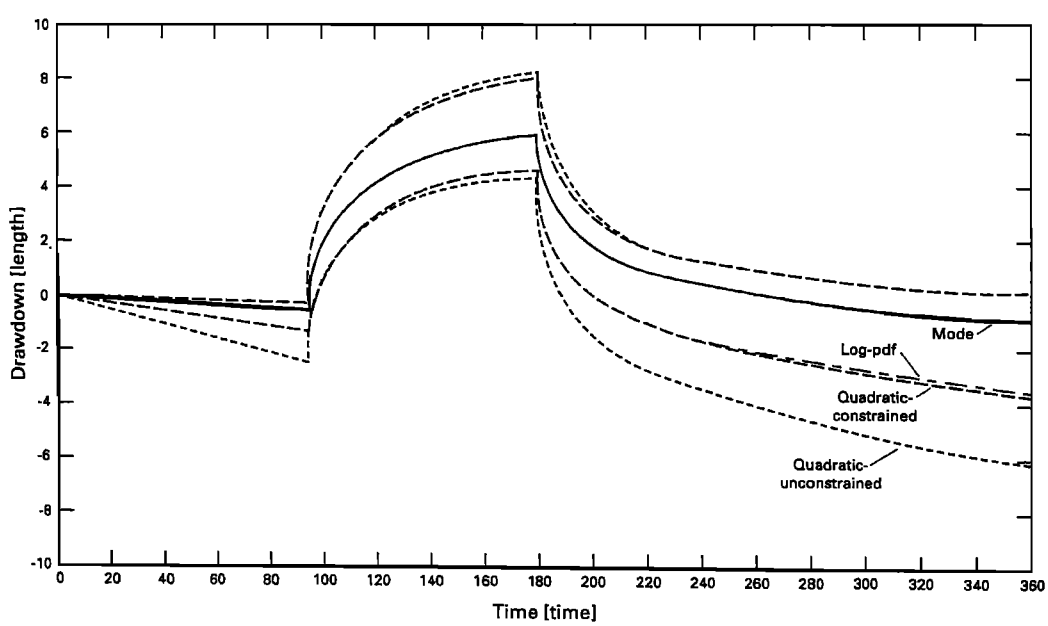

Fig. 3. Ninety-five percent confidence bands for drawdown $g(\boldsymbol{\beta})$ for the problem of flow to a well in a homogeneous aquifer (example 1), using $c \approx 1$. The mode is $g(\bar{\mathbf{b}})$.

TABLE 1. Modal Transmissivity Values for Example 2

Cell Number	ln $\bar{T}$	$\bar{T}$, (length^2/time)
1	3.00	20.086
2	3.05	21.115
3	3.10	22.198
4	3.15	23.336
5	3.20	24.533
6	3.25	25.790
7	3.30	27.113
8	3.35	28.503
9	3.40	29.964
10	3.45	31.500
11	3.50	33.115
12	3.55	34.813
13	3.60	36.598
14	3.65	38.475
15	3.70	40.447
16	3.75	42.521
17	3.80	44.701
18	3.85	46.993
19	3.90	49.402
20	3.95	51.935

because (23) shows that quadratic-unconstrained confidence intervals for the linearized model are symmetric about the point $g(\hat{\mathbf{b}})$. In this study the term nonlinear confidence intervals is used for confidence intervals that incorporate model nonlinearity, and the term linear confidence intervals is used for confidence intervals for which (B1) is employed, although these intervals may contain the nonlinear effects of parameter constraints.

Confidence intervals for the hydraulic head $g(\boldsymbol{\beta})$ at the inflow end of the aquifer for all 12 model runs are shown in Figure 4. As expected, the larger ranges (L_1, U_1) and values of c, for which parameter variances are largest, yield the largest confidence intervals. The variability in size among the confidence intervals resulting from changes in the ranges and c is quite large, probably because the ranges in T are large (over an order of magnitude) and the one-dimensional flow condition causes the hydraulic head to be very sensitive to changes in T. Asymmetry in the nonlinear confidence intervals is caused by model nonlinearity and the effects of parameter constraints, but for the linear confidence intervals, asymmetry results only from the effects of parameter constraints. As expected, both types of linear quadratic intervals tend to be more symmetric about $g(\hat{\mathbf{b}})$ than $g(\bar{\mathbf{b}})$. Except for the smallest confidence intervals (runs 1–3), all nonlinear confidence intervals tend to be asymmetric about either $g(\hat{\mathbf{b}})$ or $g(\bar{\mathbf{b}})$ but are more nearly symmetric about $g(\hat{\mathbf{b}})$. Note that there is a direct relationship between the size of the nonlinear confidence interval and its degree of asymmetry. The large degree of asymmetry for the large intervals reflects a large degree of model nonlinearity resulting from the large deviations in hydraulic head from either the expected or modal values.

TABLE 2. Models Employed for Example 2

Model Run	L_1	U_1	c	Interval Type*
1	2.9	4.05	3/11	L
2	2.9	4.05	3/11	Q-C
3	2.9	4.05	3/11	Q-U
4	2.9	4.05	0.99	L
5	2.9	4.05	1	Q-C
6	2.9	4.05	1	Q-U
7	2.3	4.4	3/11	L
8	2.3	4.4	3/11	Q-C
9	2.3	4.4	3/11	Q-U
10	2.3	4.4	0.99	L
11	2.3	4.4	1	Q-C
12	2.3	4.4	1	Q-U

*L, log pdf; Q-C, quadratic constrained; Q-U, quadratic unconstrained.

Finally, with one important exception, quadratic-unconstrained intervals are the largest of the confidence intervals, and log pdf intervals are about the same size as the corresponding quadratic-constrained intervals. The exception is run 10, which is the largest of all the intervals and is a log pdf interval. A log pdf interval larger than a corresponding quadratic-unconstrained interval was not expected and was deemed suspicious. The interval of run 10 was recalculated using the final sets of parameters produced for the upper and lower limits of the confidence interval from run 11 as the corresponding initial sets instead of the usual set $\hat{\mathbf{b}}$. Then this idea was reversed to recalculate the confidence interval for run 11. The same intervals as for runs 10 and 11 were obtained, which suggests that the interval for run 10 is correct.

Figure 1c illustrates how a log pdf interval can be larger than a quadratic-unconstrained interval for a two-parameter case. If contours of the function $g(\mathbf{b})$ were oriented such that the gradient $(\partial g/\partial b_1, \partial g/\partial b_2)$ was oriented approximately along the line $b_1 = b_2$, then the log pdf interval would be larger than either the quadratic-constrained or the quadratic-unconstrained interval.

Example 3. Two-Dimensional Steady Flow in a Multizoned Aquifer

The third and final example concerns two-dimensional, steady state flow in a realistic setting. The groundwater flow equation assumed for this example is

$$T_j\left(\frac{\partial^2 h}{\partial x^2} + \frac{\partial^2 h}{\partial y^2}\right) + R_j(H - h) + W_j + \sum_{n=1}^{N} \delta(x - x_n)\delta(y - y_n)Q_n = 0 \qquad (32)$$

where

T_j uniform transmissivity in aquifer zone j (length^2/time);

R_j uniform hydraulic conductance (hydraulic conductivity divided by thickness) of sediments underlying a stream in aquifer zone j (time^{-1});

W_j uniform areal recharge or discharge rate (positive for recharge) in aquifer zone j (length/time);

$\sum_{n=1}^{N} \delta(x - x_n)\delta(y - y_n)Q_n$ Dirac delta designation for N wells, with the nth well pumping at volumetric rate Q_n (length^3/time) (positive for injection) and located at point (x_n, y_n);

$h(x, y)$ hydraulic head in the aquifer (length);

$H(x, y)$ hydraulic head at the stream bottom (length);

x, y Cartesian coordinates (length).

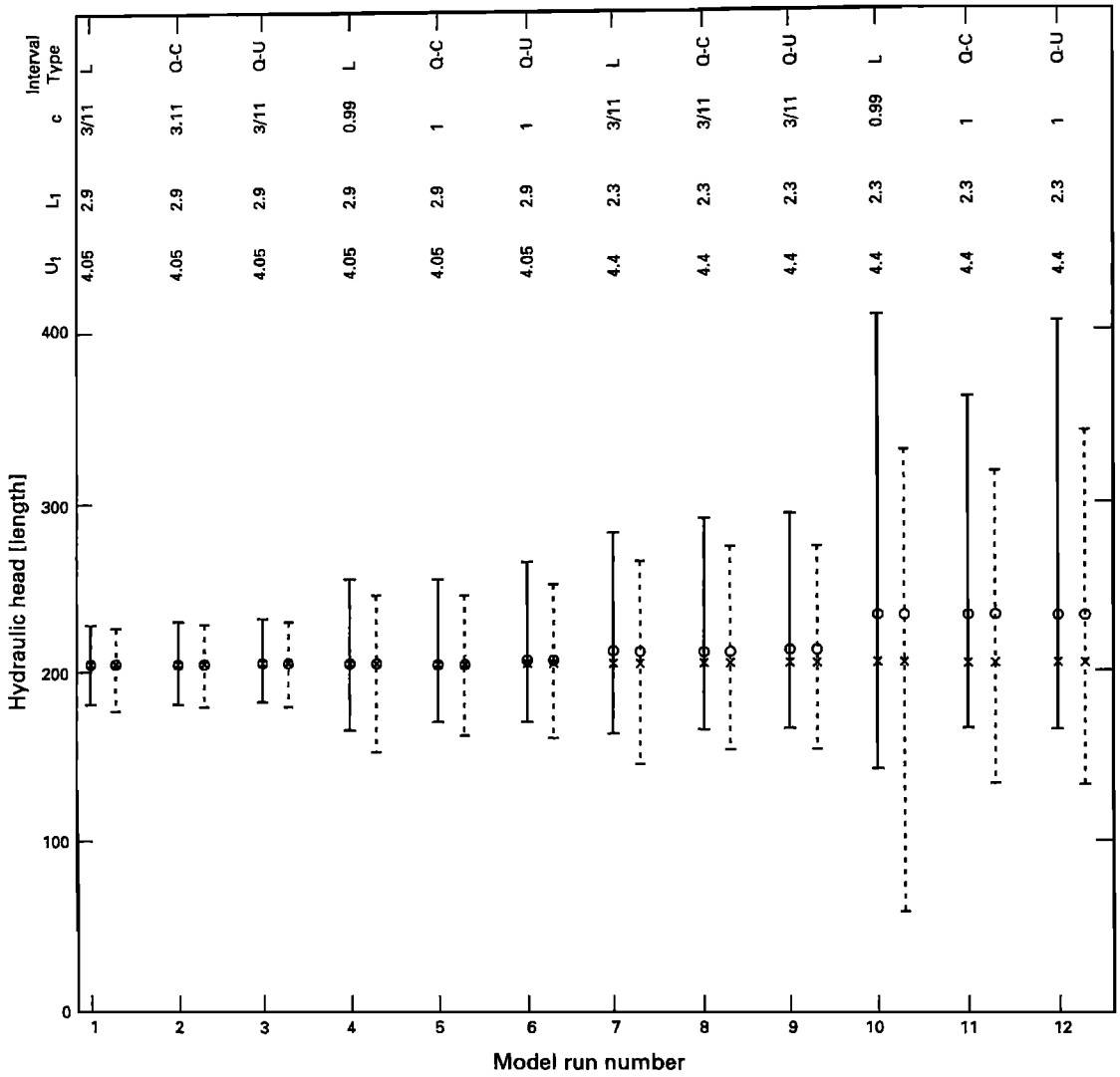

Fig. 4. Ninety-five percent confidence intervals for hydraulic head $g(\boldsymbol{\beta})$ at the inflow end of the aquifer of example 2. Open circles denote the mean $g(\hat{\mathbf{b}})$, and crosses denote the mode $g(\bar{\mathbf{b}})$. Nonlinear confidence intervals are shown as solid lines, and corresponding linear confidence intervals are shown as dashed lines.

In addition, three types of boundary conditions are employed: no flux, $q_B = 0$; specified flux q_{Bk} (length^2/time) in boundary flux zone k; and specified hydraulic head h_B. Specified head boundaries are divided into zones such that specified head parameters, say h_{Bm} and h_{Bn} (where m and n are head parameter numbers), bound the string of nodes comprising each zone within which h_B is a function of h_{Bm} and h_{Bn}. Aquifer zones, boundary flux zones, and boundary head zones are independently designated.

Numerical methods used for the solution are the same as used for the second example. The specific model geometry and zonation is illustrated in Figure 5, and modal values of parameters are given in Table 3. The parameter grouping, based solely on prior (such as measured and hydrogeologically derived) information, is shown in Table 4. Cases, which are arranged into model runs, involve two methods of specifying transmissivity parameters (ln T and T), two different values of c, and the three types of confidence intervals. Ninety-five percent confidence intervals for hydraulic head were obtained at 32 locations indicated in Figure 5 for all model runs. Representative nonlinear confidence interval widths for 11 model runs are shown in Table 5, and both nonlinear and linear confidence intervals at one location for 11 model runs are illustrated in Figure 6. The smallest set of confidence interval widths (run 1) is illustrated in Figure 7.

The six representative confidence interval widths shown in Table 5 and the illustration of confidence intervals in Figure 6 show that there is less dependence of interval size on c than for the first two examples. The largest nonlinear intervals (for run numbers 3, 6, and 9) are all of the quadratic-unconstrained type, and the remainder, which are more uniform in size, are of the other two types. This uniformity resulted because parameters having a large effect on the size of the confidence intervals were often at or near their limits for all values of c. Largely because of model nonlinearity, all nonlinear intervals are asymmetric about both $g(\hat{\mathbf{b}})$ and $g(\bar{\mathbf{b}})$; the largest intervals are the most asymmetric. Finally, log pdf intervals are similar to or slightly smaller than corresponding quadratic-constrained intervals. Thus except for the decreased dependence of interval size on c, the results are very similar to the results of example 2.

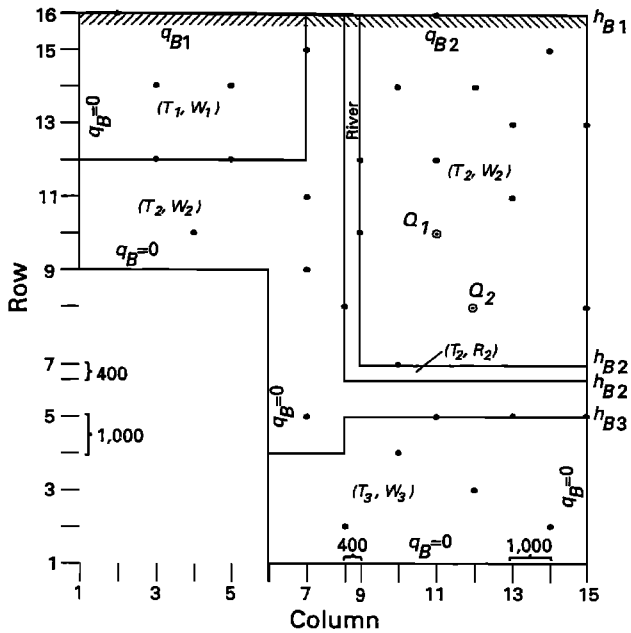

Fig. 5. Zonation and boundary conditions for example 3. Locations of confidence intervals are shown by solid circles and locations of the two pumping wells are shown by open circles. Numbers corresponding to locations are shown in Figure 7.

As indicated by comparing the nonlinear intervals for runs 3 and 9, the effect of log transformation of T for $c = 3/11$ appears to be to reduce the sizes of nonlinear quadratic-unconstrained confidence intervals. However, because of the parameter constraints, which are effectively the same for both T and ln T parameters (see Table 4), quadratic-constrained and log pdf confidence intervals are very similar for T and ln T parameters.

Solutions for nonlinear quadratic-unconstrained intervals based on untransformed transmissivities and $c = 1$ are not reported in Table 5 or illustrated in Figure 6 because transmissivity values were negative for at least one limit for 25 out of the 32 confidence intervals. The reversal of signs of transmissivities caused the signs of computed hydraulic heads (see (32)) and thus the signs of computed confidence limits to reverse. This, in turn, caused the width of the confidence intervals to be negative, which is physically impossible.

TABLE 3. Modal Values of Parameters for Example 3

Parameter	Mode
q_{B1}	0.50 (length^2/time)
q_{B2}	0.28 (length^2/time)
Q_1	−100,000 (length^3/time)
Q_2	−50,000 (length^3/time)
h_{B1}	10 (length)
h_{B2}	5 (length)
h_{B3}	5.5 (length)
T_3	20* (length^2/time)
T_1	50* (length^2/time)
T_2	500* (length^2/time)
W_3	0.0002 (length/time)
W_1	0.0003 (length/time)
W_2	−0.0001 (length/time)
R_2	0.10 (time^{-1})

*Here ln $\tilde{T}_3$ = 2.9957, ln $\tilde{T}_1$ = 3.9120, and ln $\tilde{T}_2$ = 6.2146.

The pattern of confidence intervals shown in Figure 7 reflects the differing flow conditions in various parts of the model area. Near the river and the specified head boundaries, confidence intervals are very small, whereas near the pumping wells, near the southern boundary in zone 3, and on the northwest boundary in zone 1 they are large. These relationships can be explained by noting that large confidence intervals occur wherever h is free to vary in response to flux changes and wherever the total specified flux is large relative to transmissivity. Head is constrained at or near specified head boundaries and, because R_2 is large, near the river, so confidence intervals in these areas are small. In contrast, at the pumping wells, relative specified fluxes Q_1/T_2 and Q_2/T_2 are large; in zone 3 the ratio of recharge to transmissivity (W_3/T_3) is larger in absolute value than any other zonal ratio; and on the northwest boundary the combined effect of the relative specified fluxes q_{B1}/T_1 and W_1/T_1 is large. Forcing functions of the type Q/T, W/T, and q_B/T appear to have a predominant effect on the size of the confidence intervals, and this effect will be explored further in part 2 of this study.

DISCUSSION

Calculation of the confidence limits generally proved to be very efficient for all three types of confidence intervals. Often only between two and five outer iterations were needed for convergence, and most limits were obtained with less than 10 outer iterations. However, in a few cases, convergence was difficult to obtain and, rarely, could not be obtained with a reasonable number of iterations. In the difficult cases the maximum parameter displacement $e_{\max}$ of *Cooley and Vecchia* [1987, pp. 588–589] had to be reduced to 0.5 or less, and (or) the value of $s_{1-\alpha}$ had to be increased in steps from a small value to its final correct value.

If numerous confidence intervals were desired for a large numerical model, then considerable computational effort would be required. This effort could be considerably reduced by approximating the nonlinear function $g(\mathbf{b})$ to second order, such as was done by *Townley* [1984]. In this way, approximate confidence intervals that are better than linear approximations could be obtained. *Townley* [1984] obtained good correspondence of model output means computed by the second-order method and those computed by Monte Carlo methods, so the approximation could often be good. The second-order approximation is still nonlinear in $\mathbf{b}$, so the methods used here would still be required to compute the confidence intervals.

The assumption that the most extreme values of $g(\mathbf{b})$ lie on the contour $S(\mathbf{b}) = s_{1-\alpha}$ and not in the interior of this region might seem to be very limiting. However, if this possibility is suspected, then $s_{1-\alpha}$ can be increased in steps from an initial small value to its final correct value. If an interior extreme value of $g(\mathbf{b})$ is present, then the sequence of values of $g(\mathbf{b})$ computed using the intermediate values of $s_{1-\alpha}$ should reflect its presence. In fact, $s_{1-\alpha}$ could be varied manually to approximate the extreme value. This is similar in principle to procedures used for general penalty function methods [*Himmelblau*, 1972, pp. 307–330] and could be formalized if necessary. The manual procedure was used to search for interior extreme values for several sample runs, and none were ever found. Furthermore, this writer does not believe that the condition $\partial g/\partial \mathbf{b} = \mathbf{0}$ inside of the $S(\mathbf{b}) = s_{1-\alpha}$ region

TABLE 4. Parameter Grouping Based on Prior Information for Example 3

Group Number, l	Number in Group	Parameter	Range*	L_l	U_l
1	1	q_{B1}	± 20%	0.4	0.6
2	1	q_{B2}	± 20%	0.224	0.336
3	1	Q_1	± 6%	−106,000	−94,000
4	1	Q_2	± 6%	−53,000	−47,000
5	1	h_{B1}	± 1 (length)	9	11
6	2	h_{B2}, h_{B3}	± 1 (length)	4	6.5
7	1	T_3	± 20%†	10.986‡	36.411‡
8	1	T_1	± 15%†	27.805‡	89.912‡
9	1	T_2	± 10%†	268.58‡	930.82‡
10	1	W_3	± 20%	0.00016	0.00024
11	1	W_1	± 20%	0.00024	0.00036
12	1	W_2	± 20%	−0.00012	−0.00008
13	1	R_2	± 20%	0.08	0.12

*Given as either percentage or actual deviation from the mode.
†Given as percentage deviation of logarithms of limits from $\ln \bar{T}_j$.
‡Given as transmissivity T. Values for $\ln T$ are, for $l = 7$ (2.3966, 3.5949), for $l = 8$ (3.3252, 4.4988), and for $l = 9$ (5.5931, 6.8361).

will be common for most functions $g(\mathbf{b})$ of interest in modeling studies. If this condition were to exist, then the stationary point still might not represent a value more extreme than occurs on the contour.

Another potential problem concerns the possibility of multiple stationary points for (31). This is a consequence of model nonlinearity and is shared by other schemes for finding extreme values of nonlinear functions [*Seber and Wild*, 1989, pp. 91–92]. If it is suspected that a local extreme value (and not the global extreme) of $g(\mathbf{b})$ has been obtained, then the initial parameters can be changed to see if a different extreme value of $g(\mathbf{b})$ is obtained. This procedure was used in several instances where the nonlinear confidence intervals were appreciably different from the linear intervals. In all cases it appeared that the global minimum was obtained in the original run.

Consideration of the theory and examples used for this study indicate that widths of confidence intervals for $g(\boldsymbol{\beta})$ are controlled by an interaction of (1) the size and shape of the $(1 - \alpha)$ 100% confidence region for $\boldsymbol{\beta}$, (2) whether the quadratic-constrained confidence region for $\boldsymbol{\beta}$ is being approximated by a quadratic-unconstrained confidence region for $\boldsymbol{\beta}$, and (3) the variability and degree of nonlinearity of $g(\mathbf{b})$ over the parameter space. In turn, the size and shape of the confidence region for $\boldsymbol{\beta}$ are controlled by the type of confidence region (quadratic constrained or log pdf), the size and shape of the parameter constraint boundary, the modal values of the parameters, and the peakedness parameter of the statistical distribution. Furthermore, the size and shape of the parameter constraint boundary, the modal values of the parameters, and the peakedness parameter collectively determine the parameter covariance matrix, which thus becomes an important summary control on the confidence intervals. However, in example 3, parameter constraints caused similar confidence intervals to be computed even when the values of the peakedness parameter and thus the magnitudes of the variances were different, which illustrates the point that parameter constraints are the ultimate control on widths of confidence intervals.

Quadratic-constrained and log pdf confidence intervals for $g(\boldsymbol{\beta})$ were often found to be similar for the examples, which implies similar positions of contours $S(\mathbf{b}) = s_{1-\alpha}$ for these two interval types in the vicinity of the maxima and minima of $g(\mathbf{b})$ on these contours. However, in example 2 a log pdf confidence interval was much larger than either the corresponding quadratic-constrained or quadratic-unconstrained confidence interval, and Figure 1*c* shows how this could be accounted for by interaction of the gradient of $g(\mathbf{b})$ with the size and shape of the confidence region for $\boldsymbol{\beta}$. This example demonstrates an important point: Because it is generally not

TABLE 5. Models Employed and Respresentative Confidence Interval Widths for Example 3

Run Number	c	Interval Type*	Log T	Location Number 3	5	10	14	16	31
1	3/11	L	yes	79.26	3.59	0.03	11.61	122.52	103.23
2	3/11	Q-C	yes	94.08	4.25	0.04	13.44	137.10	118.70
3	3/11	Q-U	yes	109.44	4.76	0.04	14.76	190.03	140.84
4	0.99	L	yes	96.11	4.72	0.05	16.37	138.10	138.20
5	1	Q-C	yes	96.63	4.84	0.06	16.83	138.72	140.65
6	1	Q-U	yes	260.58	10.97	0.09	32.63	453.28	327.95
7	3/11	L	no	80.93	3.67	0.03	11.89	124.80	105.41
8	3/11	Q-C	no	93.01	4.27	0.03	13.74	136.32	121.04
9	3/11	Q-U	no	314.91	13.97	0.03	36.54	700.00	373.08
10	0.99	L	no	96.24	4.75	0.05	16.48	138.19	138.90
11	1	Q-C	no	96.63	4.84	0.06	16.83	138.71	140.65

*L, log pdf; Q-C, quadratic constrained; Q-U, quadratic unconstrained.

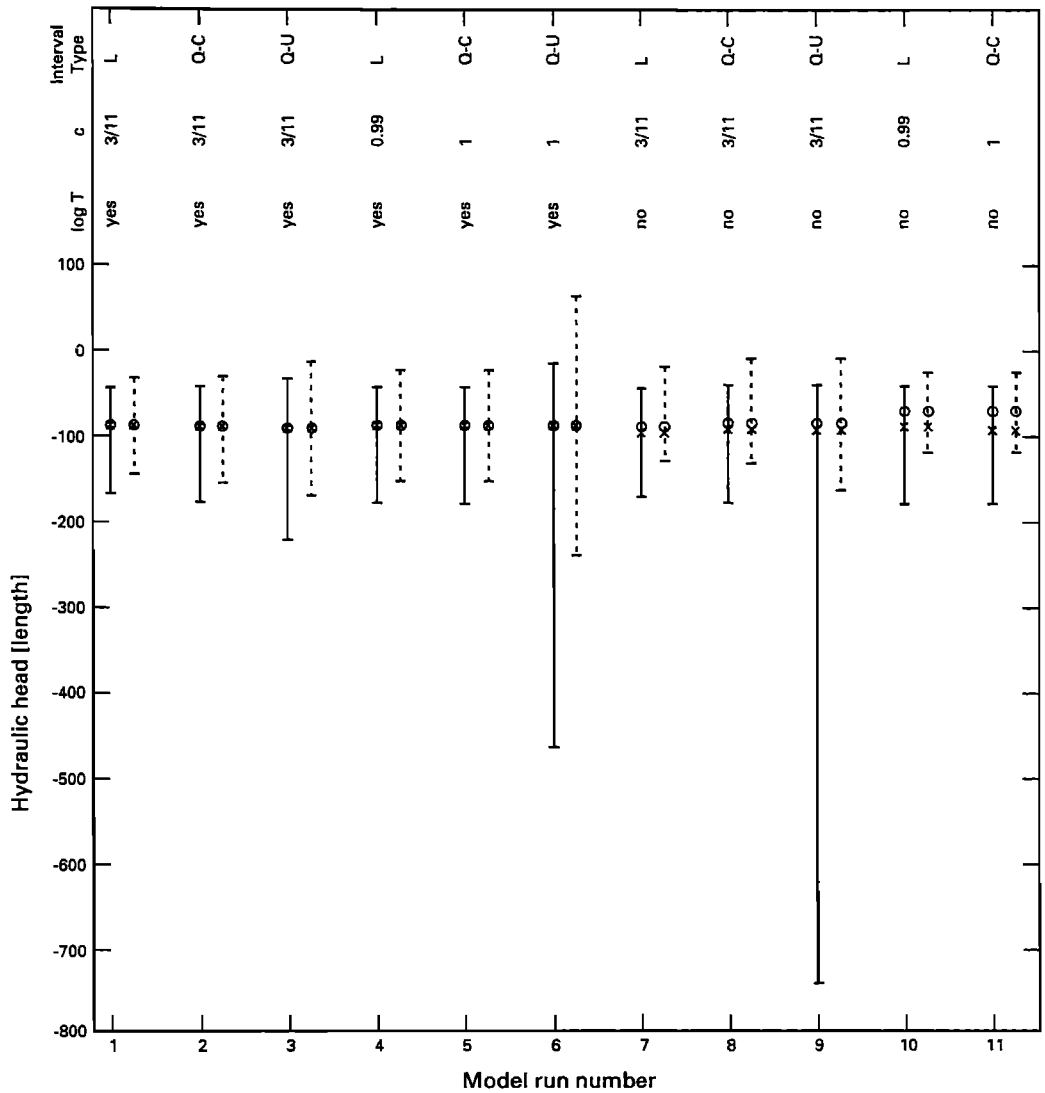

Fig. 6. Ninety-five percent confidence intervals for hydraulic head $g(\boldsymbol{\beta})$ at location 16 for example 3. Open circles denote the mean $g(\hat{\mathbf{b}})$, and crosses denote the mode $g(\bar{\mathbf{b}})$. Nonlinear confidence intervals are shown as solid lines, and corresponding linear confidence intervals are shown as dashed lines.

possible to predict the outcome of interactions of $g(\mathbf{b})$ with confidence region shapes and sizes, it is generally not possible to predict which type of confidence interval (quadratic constrained or log pdf) would be smallest in any specific instance. Both types of confidence intervals are exact and, for a particular function $g(\mathbf{b})$, differ only because of differences in the underlying confidence region for $\boldsymbol{\beta}$.

Large confidence intervals for $g(\boldsymbol{\beta})$ were often computed for the examples. For example 3 the largest confidence intervals were computed at locations where stress on the aquifer and the resulting hydraulic gradients were largest. The reason for this can be understood by examining (19). From (19), note that the magnitude of $\mathbf{b}_e - \hat{\mathbf{b}}$ (which is directly proportional to the size of the confidence intervals for $g(\boldsymbol{\beta})$) is directly proportional to the magnitude of $\mathbf{Z}$, which is the vector of sensitivities (or gradient) $\partial g/\partial \mathbf{b}$. Thus because sensitivities are large for parameters involved in producing large stresses, large stresses tend to produce large confidence intervals. Equation (19) also shows that the magnitude of $\mathbf{b}_e - \hat{\mathbf{b}}$ is directly related to the parameter covariance matrix, so that by manipulating this matrix, confidence interval widths can be reduced appreciably. This is the topic of part 2 of this study.

SUMMARY AND CONCLUSIONS

A new method was developed to compute exact confidence intervals for some function of parameters $g(\boldsymbol{\beta})$ derived from a groundwater flow model. This method requires parameters to lie within the specified parameter constraint region and so is an improvement on the original method of *Cooley and Vecchia* [1987], which can compute conservative confidence intervals because it uses parameter sets that can lie outside of the parameter constraint region. The method computes maximum and minimum limits of $g(\boldsymbol{\beta})$ on a linear combination of (1) the quadratic form for the parameters used by *Cooley and Vecchia* [1987] and (2) the log pdf contour of the assumed statistical parameter distribution of *Cooley and Vecchia* [1987]. Confidence intervals based entirely on the quadratic form with parameter constraints are

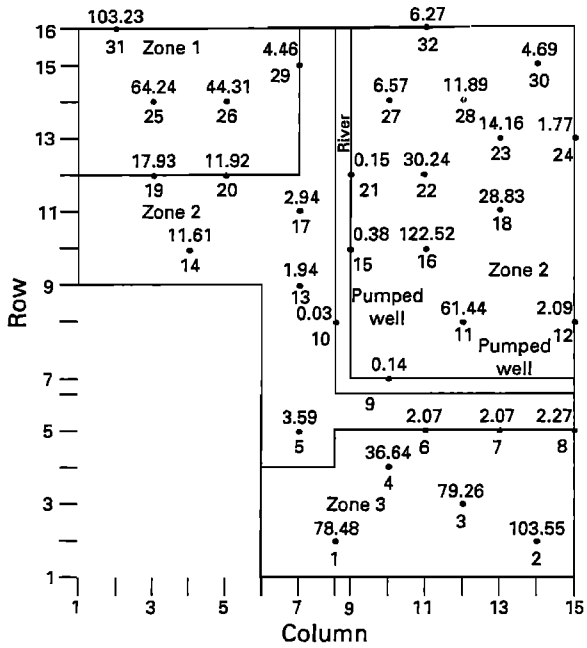

Fig. 7. Location numbers and widths of 95% confidence intervals for hydraulic head at the locations for run 1 of example 3.

called quadratic-constrained intervals, and confidence intervals based entirely on the log pdf function are called log pdf intervals. Confidence intervals produced by the original method are called quadratic-unconstrained intervals.

Three example problems demonstrate several characteristics of confidence intervals for hydraulic head $g(\boldsymbol{\beta})$ at selected points in the modeled regions. The nonlinear confidence intervals for the three examples tend to be asymmetric about both $g(\bar{\mathbf{b}})$ and $g(\hat{\mathbf{b}})$, in which $\bar{\mathbf{b}}$ is the modal parameter set and $\hat{\mathbf{b}}$ is the expected value parameter set, and the degree of asymmetry increases with the size of the interval. Comparison of confidence intervals for nonlinear and linearized models shows that the large degree of asymmetry can be attributed to the nonlinearity of the dependent variable (hydraulic head) as a function of the parameters rather than the effects of parameter constraints. Quadratic-constrained and log pdf intervals are generally similar, and quadratic-unconstrained intervals are generally much larger, although in one instance for the second example the log pdf interval is the largest of all three. The sizes of the confidence intervals are controlled by an interaction of the variability and degree of nonlinearity of $g(\mathbf{b})$ over parameter space with the size and shape of the confidence region for $\boldsymbol{\beta}$.

APPENDIX A: EVALUATION OF MODE

The modal set of parameters $\bar{\mathbf{b}}$ is the set that makes $f_{\mathbf{B}}(\mathbf{b})$ a maximum. Hence to find this set we may minimize $P'(\mathbf{b})$ defined by (25) or, more simply, $P(\mathbf{b})$ defined by (26), with respect to $\mathbf{b}$. It follows that the modal set satisfies the relationships

$$\frac{n_{lj}-1}{\bar{b}_{l,j+1}-\bar{b}_{lj}}-\frac{n_{l,j-1}-1}{\bar{b}_{lj}-\bar{b}_{l,j-1}}=0 \qquad \text{(A1)}$$

$$j=1,2,\cdots,p_l \qquad l=1,2,\cdots,k$$

or, by making use of (5),

$$\frac{C_l(\hat{b}_{l,j+1}-\hat{b}_{lj})-1}{\bar{b}_{l,j+1}-\bar{b}_{lj}}=\frac{C_l(\hat{b}_{lj}-b_{l,j-1})-1}{\bar{b}_{lj}-\bar{b}_{l,j-1}} \qquad \text{(A2)}$$

where $\bar{b}_{l0}=\hat{b}_{l0}=L_l$, $\bar{b}_{l,p_l+1}=\hat{b}_{l,p_l+1}=U_l$, $n_{l0}=m_{l1}$, and

$$C_l=\frac{1-c_l^*}{c_l^*(U_l-L_l)} \qquad \text{(A3)}$$

From (A2) it follows that

$$P_l(\bar{b}_{l,j+1}-\bar{b}_{lj})=C_l(\hat{b}_{l,j+1}-\hat{b}_{lj})-1 \qquad \text{(A4)}$$

$$j=0,1,2,\cdots,p_l$$

where P_l is a proportionality constant. To determine P_l, sum (A4) over all j, including zero, to obtain

$$\sum_{j=0}^{p_l} P_l(\bar{b}_{l,j+1}-\bar{b}_{lj})=\sum_{j=0}^{p_l}[C_l(\hat{b}_{l,j+1}-\hat{b}_{lj})-1]$$

which can be expressed as

$$P_l(U_l-L_l)=C_l(U_l-L_l)-p_l-1$$

from which, using (A3) and (6),

$$P_l=\frac{(1-c)(p_l+2)}{c(U_l-L_l)} \qquad \text{(A5)}$$

To derive the final equation relating $\hat{b}_{lj}$ to $\bar{b}_{lj}$, equations of the form of (A4) are again summed to obtain

$$\sum_{i=1}^{j} P_l(\bar{b}_{li}-\bar{b}_{l,i-1})=\sum_{i=1}^{j}[C_l(\hat{b}_{li}-\hat{b}_{l,i-1})-1]$$

Hence it follows that

$$P_l(\bar{b}_{lj}-L_l)=C_l(\hat{b}_{lj}-L_l)-j$$

or

$$\hat{b}_{lj}=\frac{P_l(\bar{b}_{lj}-L_l)+j}{C_l}+L_l \qquad \text{(A6)}$$

which, when the definitions of C_l and P_l are used, is identical to (9).

APPENDIX B: SOLUTION OF (31)

There are two sources of nonlinearity with respect to $\mathbf{b}$ in (31), one from the function $g(\mathbf{b})$ and the other from the function $P(\mathbf{b})$. The method of solving (31) described in this section is a variant of Newton iteration that deals with these two sources separately. The iterative solution is obtained with an inner iteration loop in which $g(\mathbf{b})$ is treated as if it were linear in $\mathbf{b}$ (that is, $\partial g/\partial \mathbf{b}$ is held constant) and an outer loop in which this source of nonlinearity is incorporated. Separate parameter sets are used for inner and outer iterations to facilitate description of the method. In the following development the parameter set calculated at the end of the previous outer iteration is designated $\mathbf{b}_0$, and the parameter set calculated at the end of the previous inner iteration is

designated $\mathbf{b}_1$. All variables calculated using one or the other of these parameter sets have a superscript or subscript 0 or 1, as appropriate.

To develop an algorithm to solve (31), first replace $g(\mathbf{b})$ in (31) with the linearized model

$$g(\mathbf{b}) \simeq g(\mathbf{b}_0) + \mathbf{Z}_0^T(\mathbf{b} - \mathbf{b}_0) \tag{B1}$$

which is obtained by expanding $g(\mathbf{b})$ in a Taylor series about $\mathbf{b}_0$ and retaining only first-order terms. In (B1), column vector $\mathbf{Z}_0$ is defined by

$$\mathbf{Z}_0 = \left\{\frac{\partial g}{\partial b_{lj}}\right\}_{\mathbf{b} = \mathbf{b}_0} \tag{B2}$$

Second, obtain a quadratic approximation of $S(\mathbf{b})$ by expanding $S(\mathbf{b})$ in a Taylor series about $\mathbf{b}_1$ and retaining only first- and second-order terms:

$$S(\mathbf{b}) \simeq S_1 + \sum_{l=1}^{k} \mathbf{G}_l^{1T}\boldsymbol{\delta}_l + \frac{1}{2}\sum_{l=1}^{k} \boldsymbol{\delta}_l^T\mathbf{H}_l^1\boldsymbol{\delta}_l \tag{B3}$$

where $S_1 = S(\mathbf{b}_1)$,

$$\mathbf{G}_l^1 = a\mathbf{V}_l^{-1}(\mathbf{b}_l^1 - \hat{\mathbf{b}}_l) + b\mathbf{v}_l^1 \tag{B4}$$

$$\mathbf{H}_l^1 = a\mathbf{V}_l^{-1} + b\mathbf{D}_l^1 \tag{B5}$$

$$\boldsymbol{\delta}_l = \mathbf{b}_l - \mathbf{b}_l^1 \tag{B6}$$

In (B4) $\mathbf{v}_l^1$ is a vector composed of elements

$$v_{lj}^1 = \frac{n_{lj} - 1}{b_{l,j+1}^1 - b_{lj}^1} - \frac{n_{l,j-1}}{b_{lj}^1 - b_{l,j-1}^1} \tag{B7}$$

and in (B5) $\mathbf{D}_l^1$ is a symmetric, tridiagonal, positive definite coefficient matrix in which row j is composed of the following nonzero elements:

$$D_{l,j-1}^1 = -\frac{n_{l,j-1} - 1}{(b_{lj}^1 - b_{l,j-1}^1)^2}$$

$$D_{lj}^1 = \frac{n_{l,j-1} - 1}{(b_{lj}^1 - b_{l,j-1}^1)^2} + \frac{n_{lj} - 1}{(b_{l,j+1}^1 - b_{lj}^1)^2} \tag{B8}$$

$$D_{l,j+1}^1 = -\frac{n_{lj} - 1}{(b_{l,j+1}^1 - b_{lj}^1)^2}$$

In (B8) the usual matrix double index has been suppressed for simplicity. Matrix $\mathbf{D}_l^1$ is positive definite because it is a Stieltjes matrix [*Varga*, 1962, p. 85].

Equation (B3) may be simplified by defining $\mathbf{G}_1 = (\mathbf{G}_1^{1T}, \mathbf{G}_2^{1T}, \cdots, \mathbf{G}_k^{1T})^T$, $\boldsymbol{\delta} = (\boldsymbol{\delta}_1^T, \boldsymbol{\delta}_2^T, \cdots, \boldsymbol{\delta}_k^T)^T$, and $\mathbf{H}_1 = \operatorname{diag}(\mathbf{H}_1^1, \mathbf{H}_2^1, \cdots, \mathbf{H}_k^1)$. Then, from (B3),

$$S(\mathbf{b}) = S_1 + \mathbf{G}_1^T\boldsymbol{\delta} + \tfrac{1}{2}\boldsymbol{\delta}^T\mathbf{H}_1\boldsymbol{\delta} \tag{B9}$$

Vector $\mathbf{G}_1$ is the gradient of $S(\mathbf{b})$, and matrix $\mathbf{H}_1$ is the positive definite Hessian of $S(\mathbf{b})$, both evaluated at point $\mathbf{b}_1$.

Third, substitute (B1) and (B9) into (31), take the derivative of the resulting equation with respect to $\mathbf{b}$ and λ_p', and set the results to zero to obtain the equations used to calculate the correction $\boldsymbol{\delta}$ to approximate extreme value set $\mathbf{b}_1$ based on the approximations (B1) and (B9). The equations are

$$\mathbf{H}_1\boldsymbol{\delta} = \lambda_p\mathbf{Z}_0 - \mathbf{G}_1 \tag{B10}$$

$$\tfrac{1}{2}\boldsymbol{\delta}^T\mathbf{H}_1\boldsymbol{\delta} + \mathbf{G}_1^T\boldsymbol{\delta} + S_1 = s_{1-\alpha} \tag{B11}$$

where $\lambda_p = 1/\lambda_p'$.

To solve for λ_p, first solve (B10) for $\boldsymbol{\delta}$ and substitute this result into (B11) to get

$$\tfrac{1}{2}(\lambda_p\mathbf{Z}_0 + \mathbf{G}_1)^T\mathbf{H}_1^{-1}(\lambda_p\mathbf{Z}_0 - \mathbf{G}_1) + S_1 = s_{1-\alpha} \tag{B12}$$

Next solve (B12) for λ_p to obtain

$$\lambda_p = \pm\left(\frac{2(s_{1-\alpha} - S_1) + \mathbf{G}_1^T\mathbf{H}_1^{-1}\mathbf{G}_1}{\mathbf{Z}_0^T\mathbf{H}_1^{-1}\mathbf{Z}_0}\right)^{1/2} \tag{B13}$$

It is proven later that use of the plus sign leads to the upper confidence limit $g(\mathbf{b}_e)$ and use of the minus sign leads to the lower confidence limit. Note that because $\mathbf{H}_1$ is positive definite, both quadratic forms in (B13) are positive or zero. Thus if $\mathbf{b}_1$ is within the feasible region $S_1 \leq s_{1-\alpha}$, and $\mathbf{Z}_0 \neq \mathbf{0}$, λ_p is always real and finite.

To efficiently employ (B10) and (B13) to solve for $\boldsymbol{\delta}$, decompose (B10) into two problems and use these solutions in (B13) as follows:

$$\boldsymbol{\delta}_Z = \mathbf{H}_1^{-1}\mathbf{Z}_0 \tag{B14}$$

$$\boldsymbol{\delta}_V = \mathbf{H}_1^{-1}\mathbf{G}_1 \tag{B15}$$

so that

$$\lambda_p = \pm\left(\frac{2(s_{1-\alpha} - S_1) + \mathbf{G}_1^T\boldsymbol{\delta}_V}{\mathbf{Z}_0^T\boldsymbol{\delta}_Z}\right)^{1/2} \tag{B16}$$

$$\boldsymbol{\delta} = \lambda_p\boldsymbol{\delta}_Z - \boldsymbol{\delta}_V \tag{B17}$$

It was found that an algorithm based directly on (B14)–(B17) generated unacceptable round-off error whenever the log pdf contour $S(\mathbf{b})$ was very near the boundary of the parameter region. Small differences of the type $b_{lj}^1 - b_{l,j-1}^1$ appearing in S_1, $\mathbf{v}_l^1$, and $\mathbf{D}_l^1$ could not be computed accurately enough to obtain the solution. Hence equations in which these differences appear are written in terms of the variable

$$d_{lj}^1 = b_{lj}^1 - b_{l,j-1}^1 \tag{B18}$$

New values of the parameter difference, $d_{lj} = b_{lj}^e - b_{l,j-1}^e$, are computed as follows. First, obtain $\boldsymbol{\delta}_Z$ and $\boldsymbol{\delta}_V$ from (B14) and (B15). Next, for $j = 1, 2, \cdots, p_l$ and $l = 1, 2, \cdots, k$ form

$$w_{lj}^V = \delta_{lj}^V - \delta_{l,j-1}^V \tag{B19}$$

$$w_{lj}^Z = \delta_{lj}^Z - \delta_{l,j-1}^Z \tag{B20}$$

so that, based on (B17),

$$w_{lj} = \lambda_p w_{lj}^Z - w_{lj}^V \tag{B21}$$

where $\delta_{l0}^V = \delta_{l0}^Z = 0$. Finally, compute d_{lj} from

$$d_{lj} = \rho_c w_{lj} + d^1_{lj} \tag{B22}$$

where ρ_c ($0 < \rho_c \leq 1$) is a damping parameter. New parameter set $\mathbf{b}_e$ is computed by solving $b^e_{lj} = d_{lj} + b^e_{l,j-1}$ recursively for each group l, starting with $b^e_{l1} = d_{l1} + L_l$.

Damping parameter ρ_c is employed to keep updated parameter sets $\mathbf{b}_e$ within constraint boundary (1). It is computed using the following method. Set $\rho_{lj} = 1 (j = 1, 2, \cdots, p_l + 1; l = 1, 2, \cdots, k)$. If $b^1_{l1} + \delta_{l1} < L_l$, then compute ρ_{l1} so that $b^1_{l1} + \rho_{l1}\delta_{l1} = L_l$, or

$$\rho_{l1} = \frac{L_l - b^1_{l1}}{\delta_{l1}} = \frac{-d^1_{l1}}{\delta_{l1}} = \frac{-d^1_{l1}}{w_{l1}} \tag{B23}$$

If $b^1_{l,j+1} + \delta_{l,j+1} < b^1_{lj} + \delta_{lj}$ for any j ($j = 1, 2, \cdots, p_l - 1$), then compute $\rho_{l,j+1}$ so that $b^1_{l,j+1} + \rho_{l,j+1}\delta_{l,j+1} = b^1_{lj} + \rho_{l,j+1}\delta_{lj}$, or

$$\rho_{l,j+1} = \frac{b^1_{l,j+1} - b^1_{lj}}{\delta_{lj} - \delta_{l,j+1}} = \frac{d^1_{l,j+1}}{\delta_{lj} - \delta_{l,j+1}} = \frac{-d^1_{l,j+1}}{w_{l,j+1}} \tag{B24}$$

If $b^1_{lp_l} + \delta_{lp_l} > U_l$, then compute ρ_{l,p_l+1} so that $b^1_{lp_l} + \rho_{l,p_l+1}\delta_{lp_l} = U_l$, or

$$\rho_{l,p_l+1} = \frac{U_l - b^1_{lp_l}}{\delta_{lp_l}} = \frac{d^1_{l,p_l+1}}{\delta_{lp_l}} = \frac{-d^1_{l,p_l+1}}{w_{l,p_l+1}} \tag{B25}$$

Finally, if $\min_{l,j} \rho_{lj} = 1$, set $\rho_c = 1$, and if $\min_{l,j} \rho_{lj} < 1$, compute

$$\rho_c = 0.999 \min_{l,j} \rho_{lj} \tag{B26}$$

where the factor of 0.999 is needed because $\min_{l,j} \rho_{lj} < 1$ implies that at least one constraint is exactly satisfied, which would result in taking the log of zero when computing $S(\mathbf{d})$. To avoid this problem, ρ_c must be less than $\min_{l,j} \rho_{lj}$; the exact value of 0.999 is arbitrary.

Because λ_p is computed using (B16) before ρ_c is computed, parameters implied by $\boldsymbol{\delta}_Z$ and $\boldsymbol{\delta}_V$ from (B14) and (B15) may lie outside of the constraint boundary so that $S(\mathbf{b}_e) > s_{1-\alpha}$, which can lead to an imaginary value for λ_p. It is sufficient to check the numerator of (B16) to see if it is positive. If it is not, then λ_p may be set to zero, which ensures a step $\boldsymbol{\delta}$ such that, with sufficient damping, $S(\mathbf{b})$ can be reduced. To prove this, note that $\mathbf{G}_1$ is the gradient of $S(\mathbf{b})$ at $\mathbf{b} = \mathbf{b}_1$ and that, with $\lambda_p = 0$, (B10) becomes

$$\mathbf{H}_1\boldsymbol{\delta} = -\mathbf{G}_1 \tag{B27}$$

Premultiply (B27) by $\boldsymbol{\delta}^T$ to obtain

$$\boldsymbol{\delta}^T\mathbf{H}_1\boldsymbol{\delta} = -\boldsymbol{\delta}^T\mathbf{G}_1 > 0 \tag{B28}$$

where the inequality follows because $\mathbf{H}_1$ is positive definite. The term $-\boldsymbol{\delta}^T\mathbf{G}_1$ is the dot product of the negative of the gradient vector and the vector of changes in parameters. Because this dot product is positive, the angle between the two vectors is less than 90°. Therefore with sufficient damping $S(\mathbf{b})$ can be reduced compared to S_1, as is required.

Convergence of the inner iteration loop is indicated by small absolute values in $\boldsymbol{\delta}$, and convergence of the outer loop is indicated by small absolute changes in $\mathbf{b}_e$ (that is, $\mathbf{b}_e \simeq \mathbf{b}_0$) over the outer loop. Damping used in the inner iteration loop is given by (B23)–(B26). Damping used in the outer iteration loop is given by the algorithm of *Cooley and Vecchia* [1987, pp. 588–589] with the exception that here the damping parameter is set to unity on the first iteration.

In summary, the algorithm used to solve (31) for the upper ($\lambda_p > 0$) confidence limit $g(\mathbf{b}_e)$ is as follows. (The algorithm for the lower confidence limit is identical except the negative value of λ_p is used.)

1. Define an initial set of parameters $\mathbf{b}_1$ and set $\mathbf{b}_0 = \mathbf{b}_1$.
2. Compute $\mathbf{Z}_0$.
3. Compute $\mathbf{H}_1$, $\mathbf{G}_1$, and S_1 using (B18) for parameter differences.
4. Compute $\boldsymbol{\delta}_Z$ and $\boldsymbol{\delta}_V$ using (B14) and (B15).
5. Compute λ_p using the positive value from (B16), unless the numerator of (B16) is negative, in which case $\lambda_p = 0$.
6. Compute ρ_c using (B23)–(B26).
7. Compute $\mathbf{d}$, which is the vector of elements d_{lj}, using (B19)–(B22).
8. Compute $\mathbf{b}_e$ using $\mathbf{d}$.
9. Compute $\boldsymbol{\delta}$ using (B17) and check for convergence. If $\boldsymbol{\delta}$ is not small enough, return to (3).
10. Check $|\mathbf{b}_e - \mathbf{b}_0|$ for convergence. If this difference is not small enough, then use the algorithm of *Cooley and Vecchia* [1987, pp. 588–589] to compute a new, damped parameter set $\mathbf{b}_e$; set $\mathbf{b}_0 = \mathbf{b}_e$; then return to (2). Otherwise compute the confidence limit $g(\mathbf{b}_e)$.

The condition for (B10) and (B13) to lead to a maximum of $g(\mathbf{b})$ is $g(\mathbf{b}) - g(\mathbf{b}_0) \simeq \mathbf{Z}_0^T\boldsymbol{\delta} > 0$. This condition may be specified in terms of (B10). Solve (B10) for $\boldsymbol{\delta}$ and premultiply the result by $\mathbf{Z}_0^T$ to obtain

$$g(\mathbf{b}) - g(\mathbf{b}_0) \simeq \mathbf{Z}_0^T\boldsymbol{\delta} = \mathbf{Z}_0^T\mathbf{H}_1^{-1}(\lambda_p\mathbf{Z}_0 - \mathbf{G}_1) > 0 \tag{B29}$$

Thus the condition on λ_p to lead to a maximum is

$$\lambda_p > \frac{\mathbf{Z}_0^T\mathbf{H}_1^{-1}\mathbf{G}_1}{\mathbf{Z}_0^T\mathbf{H}_1^{-1}\mathbf{Z}_0} \tag{B30}$$

It is now shown that if (1) the positive root in (B13) is used, (2) $\mathbf{Z}_0 \neq \mathbf{0}$, and (3) $S_1 < s_{1-\alpha}$, then (B30) is always true. Rearrange (B11) and rewrite it using (B10):

$$(\lambda_p\mathbf{Z}_0 + \mathbf{G}_1)^T\boldsymbol{\delta} = (\mathbf{H}_1\boldsymbol{\delta} + 2\mathbf{G}_1)^T\boldsymbol{\delta} = \boldsymbol{\delta}^T\mathbf{H}_1\boldsymbol{\delta} + 2\mathbf{G}_1^T\boldsymbol{\delta}$$
$$= 2(s_{1-\alpha} - S_1)$$

so that, because $\boldsymbol{\delta}^T\mathbf{H}_1\boldsymbol{\delta} > 0$,

$$\mathbf{G}_1^T\boldsymbol{\delta} < s_{1-\alpha} - S_1 < 2(s_{1-\alpha} - S_1)$$

or by adding $\mathbf{G}_1^T\mathbf{H}_1^{-1}\mathbf{G}_1$ to each side and using (B10) and (B13),

$$\mathbf{G}_1^T\boldsymbol{\delta} + \mathbf{G}_1^T\mathbf{H}_1^{-1}\mathbf{G}_1 = (\mathbf{H}_1\boldsymbol{\delta} + \mathbf{G}_1)^T\mathbf{H}_1^{-1}\mathbf{G}_1 = \lambda_p\mathbf{Z}_0^T\mathbf{H}_1^{-1}\mathbf{G}_1$$
$$< 2(s_{1-\alpha} - S_1) + \mathbf{G}_1^T\mathbf{H}_1^{-1}\mathbf{G}_1 = \lambda_p^2\mathbf{Z}_0^T\mathbf{H}_1^{-1}\mathbf{Z}_0$$

which is the same as (B30).

The condition for (B10) and (B13) to lead to a minimum is

$$g(\mathbf{b}) - g(\mathbf{b}_0) \simeq \mathbf{Z}_0^T\boldsymbol{\delta} = \mathbf{Z}_0^T\mathbf{H}_1^{-1}(\lambda_p\mathbf{Z}_0 - \mathbf{G}_1) < 0 \tag{B31}$$

from which the condition on λ_p is

$$\lambda_p < \frac{\mathbf{Z}_0^T \mathbf{H}_1^{-1} \mathbf{G}_1}{\mathbf{Z}_0^T \mathbf{H}_1^{-1} \mathbf{Z}_0} \tag{B32}$$

An argument similar to that developed for the maximum shows that if (1) the negative root in (B13) is used, (2) $\mathbf{Z}_0 \neq \mathbf{0}$, and (3) $S_1 < s_{1-\alpha}$, then (B32) is always true.

NOTATION

- a a constant giving the weight applied for $Q(\mathbf{B})$ in $S(\mathbf{B})$.
- b a constant giving the weight applied for $P(\mathbf{B})$ in $S(\mathbf{B})$.
- $\mathbf{B}$ a set of random variables from a statistical distribution that describes parameter uncertainty and covers the plausible range for $\boldsymbol{\beta}$; a subvector of $\mathbf{B}$ is $\mathbf{B}_l$, where l is a parameter group number.
- $\mathbf{b}$ a realization of $\mathbf{B}$; a subvector of $\mathbf{b}$ corresponding to $\mathbf{B}_l$ is $\mathbf{b}_l$.
- $\bar{\mathbf{b}}$ a fixed estimate of $\boldsymbol{\beta}$ resulting from prior (measured and subjective) information and(or) model calibration; a subvector of $\bar{\mathbf{b}}$ corresponding to $\mathbf{B}_l$ is $\bar{\mathbf{b}}_l$.
- $\hat{\mathbf{b}}$ $E(\mathbf{B})$
- $\mathbf{b}_e$ current estimate of the parameter set for which $g(\mathbf{b})$ is either a maximum or a minimum, subject to the appropriate parameter constraints.
- c peakedness parameter of the multivariate beta distribution.
- $c_l^* = c/(p_l + 2)$.
- $d_{1-\alpha}^2$ critical value of $Q(\mathbf{B})$ defined by Prob $[Q(\mathbf{B}) \leq d_{1-\alpha}^2] = 1 - \alpha$.
- $f_{\mathbf{B}}(\mathbf{b})$ prior distribution, defined by (2).
- $g(\mathbf{b})$ model output or other scalar function (of some set of parameters $\mathbf{b}$) for which a confidence interval is desired.
- k number of parameter groups.
- L_l lower parameter bound for parameter group l.
- m_{lj} exponent for multivariate beta distribution; defined as $(1 - c_l^*)(\hat{b}_{lj} - L_l)/[c_l^*(U_l - L_l)]$.
- n_{lj} exponent for multivariate beta distribution; defined as $(1 - c_l^*)(\hat{b}_{l,j+1} - \hat{b}_{lj})/[c_l^*(U_l - L_l)]$.
- p_l number of parameters in parameter group l.
- $Q(\mathbf{B}) = (\mathbf{B} - \hat{\mathbf{b}})^T \mathbf{V}^{-1} (\mathbf{B} - \hat{\mathbf{b}})$.
- $P(\mathbf{B})$ scaled log pdf function for the multivariate beta distribution of parameters, equal to $-\sum_{l=1}^{k} \sum_{j=0}^{p_l} (n_{lj} - 1) \ln ((B_{l,j+1} - B_{lj})/(U_l - L_l))$
- $S(\mathbf{B})$ linear combination $aQ(\mathbf{B}) + bP(\mathbf{B})$.
- $s_{1-\alpha}$ critical value of $S(\mathbf{B})$ defined by Prob $[S(\mathbf{B}) \leq s_{1-\alpha}] = 1 - \alpha$.
- U_l upper parameter bound for parameter group l.
- $\mathbf{V}$ Var($\mathbf{B}$); a submatrix is $\mathbf{V}_l$ = Var ($\mathbf{B}_l$).
- $\mathbf{Z}_0$ sensitivity vector (or gradient of $g(\mathbf{b})$) $\partial g/\partial \mathbf{b}|_{\mathbf{b}=\mathbf{b}_0}$, where $\mathbf{b}_0$ is the set of parameters calculated on the previous outer iteration.
- α probability that $Q(\mathbf{B})$ or $S(\mathbf{B})$ is greater than critical values of $d_{1-\alpha}^2$ or $s_{1-\alpha}$, respectively.
- $\boldsymbol{\beta}$ true but unknown set of model parameters.
- $\lambda_u = 1/(2\lambda_u')$, where λ_u' is the Lagrange multiplier for confidence intervals based on $Q(\mathbf{b})$.
- $\lambda_p = 1/\lambda_p'$, where λ_p' is the Lagrange multiplier for confidence intervals based on $S(\mathbf{b})$.

Acknowledgments. The author thanks colleague reviewers Mary C. Hill, Paul A. Hsieh, Allen M. Shapiro, Brent M. Troutman, and Aldo V. "Skip" Vecchia, Jr., for the hours spent and their many helpful comments. In addition, Skip Vecchia wrote the computer program to compute critical values $d_{1-\alpha}^2$ and $s_{1-\alpha}$, donated several hours of his time to stimulating discussions concerning the methods, and gave valuable insights into the statistical theory on which the calculation methods are based.

REFERENCES

Bates, B. C., Improved methodology for parameter inference in nonlinear, hydrologic regression models, *Water Resour. Res.*, *28*(1), 89–97, 1992.

Cooley, R. L., A comparison of several methods of solving nonlinear regression groundwater flow problems, *Water Resour. Res.*, *21*(10), 1525–1538, 1985.

Cooley, R. L., Exact Scheffé-type confidence intervals for output from groundwater flow models, 2, Combined use of hydrogeologic information and calibration data, *Water Resour. Res.*, this issue.

Cooley, R. L., and R. L. Naff, Regression modeling of ground-water flow, *Techniques of Water Resour. Invest. of the U.S. Geol. Surv.*, book 3, chap. B4, 232 pp., U.S. Geol. Surv., Reston, Va., 1990.

Cooley, R. L., and A. V. Vecchia, Calculation of nonlinear confidence and prediction intervals for ground-water flow models, *Water Resour. Bull.*, *23*(4), 581–599, 1987.

Dagan, G., Statistical theory of groundwater flow and transport: Pore to laboratory, laboratory to formation, formation to regional scale, *Water Resour. Res.*, *22*(9), 120S–134S, 1986.

Dettinger, M. D., and J. L. Wilson, First-order analysis of uncertainty in numerical models of groundwater flow, 1, Mathematical development, *Water Resour. Res.*, *17*(1), 149–161, 1981.

Gelhar, L. W., Stochastic analysis of flow in heterogeneous porous media, in *Fundamentals of Transport Phenomena in Porous Media*, edited by J. Bear and M. Y. Corapcioglu, pp. 673–720, Martinus Nijhoff, Dordrecht, Netherlands, 1984.

Gelhar, L. W., Stochastic subsurface hydrology, from theory to applications, *Water Resour. Res.*, *22*(9), 135S–145S, 1986.

Graybill, F. A., *Theory and Application of the Linear Model*, 704 pp., Duxbury Press, North Scituate, Mass., 1976.

Hill, M. C., Analysis of accuracy of approximate, simultaneous, nonlinear confidence intervals on hydraulic heads in analytical and numerical test cases, *Water Resour. Res.*, *25*(2), 177–190, 1989.

Himmelblau, D. M., *Applied Nonlinear Programming*, 497 pp., McGraw-Hill, New York, 1972.

Keidser, A., and D. Rosbjerg, A comparison of four inverse approaches to groundwater flow and transport identification, *Water Resour. Res.*, *27*(9), 2219–2232, 1991.

Konikow, L. F., Predictive accuracy of a ground-water model—Lessons from a post audit, *Ground Water*, *24*(2), 173–184, 1986.

Lehmann, E. L., *Testing Statistical Hypotheses*, 2nd ed., 600 pp., John Wiley, New York, 1986.

Rao, C. R., *Linear Statistical Inference and its Applications*, 2nd ed., 625 pp., John Wiley, New York, 1973.

Seber, G. A. F., and C. J. Wild, *Nonlinear Regression*, 768 pp., John Wiley, New York, 1989.

Sykes, J. F., J. L. Wilson, and R. W. Andrews, Sensitivity analysis for steady state groundwater flow using adjoint operators, *Water Resour. Res.*, *21*(3), 359–371, 1985.

Townley, L. R., Second order effects of uncertain transmissivities on predictions of piezometric heads, in *Finite Elements in Water Resources, Proceedings of the 5th International Conference*, edited by J. P. Laible, C. A. Brebbia, W. G. Gray, and G. F. Pinder, pp. 251–264, Springer-Verlag, New York, 1984.

Varga, R. S., *Matrix Iterative Analysis*, 322 pp., Prentice-Hall, Englewood Cliffs, N. J., 1962.

R. L. Cooley, Water Resources Division, U.S. Geological Survey, Box 25046, Mail Stop 413, Denver Federal Center, Denver, CO 80225.

(Received October 10, 1991;
revised July 31, 1992;
accepted August 7, 1992.)